Research article

JGS
Journal of the Geological Society

https://doi.org/10.1144/jgs2023-001 | Vol. 180 | 2023 | jgs2023-001

The Charnwood Terrane revisited: an integrated petrogenetic and petrophysical model for crustal structure in southern Britain

T. C. Pharaoh*, D. Beamish, J. D. O. Williams, J. N. Carney and P. R. Wilby

British Geological Survey, Keyworth, Nottingham, UK
TCP, 0000-0002-0452-5088
* Correspondence: tcp@bgs.ac.uk

Abstract: We based an integrated petrological and petrophysical model for the Ediacaran crust of southern Britain on a review of the *c.* 570–550 Ma Charnian volcano-sedimentary complex. The latter was emplaced in a magmatic rift wedge within the juvenile continental crust of the *c.* 720–600 Ma Marches Terrane, a subduction magmatic domain formed at the margin of the Gondwana palaeocontinent. The Charnian magmatic arc is characterized by primitive island arc tholeiite to more evolved calc-alkaline compositions. The inversion of aeromagnetic potential field data and petrophysical modelling reveals details of the internal structure of the Charnian Domain, including a median rift, superimposed annular structures and partitioning lineaments. The modelling suggests that the arc foundation could incorporate magnetite-rich cumulates, which may explain the anomalous geophysical properties, including crustal thickness, rigidity and buoyancy. There is no evidence for significant tectonic displacement between the Charnian Domain and its Marches Terrane host. Instead, the domain likely occupies a wedge-shaped arc/marginal rift basin complex, propagated from a neighbouring ocean into the Gondwana margin. Contemporaneous volcanic rift successions in the Welsh Borderland and Wales of the 570–550 Ma Charnian magmatic phase developed in coeval ensialic rifts within less strongly extended Marches Terrane lithosphere. A comparable diversity of subduction-related magmatism is found in the Neogene–recent Hikurangi destructive margin of New Zealand, providing a plausible analogue for Charnian magmatism.

Supplementary material: Supplementary Publication 1 (borehole geophysical log correlation; petrophysical data table; unannotated geophysical maps and sections) and Supplementary Publication 2 (geochemistry analytical conditions and data table) are available at https://doi.org/10.6084/m9.figshare.c.6805248

Received 1 January 2023; **revised** 10 July 2023; **accepted** 20 August 2023

Following Williams and Hatcher (1982), the crust of southern Britain has been compared with Ediacaran terranes scattered through the Appalachian–Caledonian Orogen between Florida and western Europe (e.g. Nance and Murphy 1996) (Fig. 1a). The crust of southern Britain forms part of the Wales–Anglo–Brabant Massif (Fig. 1a). Historically, these terranes have been assigned to the Avalonia microcontinent to discriminate them from other peri-Gondwanan terranes, such as the Cadomian Terrane (or assemblage), within the Variscan–Alleghenian Orogen that have a slightly different history and provenance. There is an ongoing debate about the correlation of the crust in southern Britain, which was incorporated into the Caledonian Orogen in the late Ordovician–early Silurian, with that of the Avalon Terrane in its type area in Newfoundland and the Maritime Provinces of Canada (the so-called Western Avalonia) within the Appalachian Orogen.

Previous models for the Neoproterozoic crustal evolution of southern Britain have focused on the role of magmatic processes (e.g. Thorpe *et al.* 1984; Pharaoh *et al.* 1987; Schofield *et al.* 2016) and strike-slip displacement (e.g. Gibbons 1987, 1990; Gibbons and Horák 1996) during subsequent accretion and dispersal within the Iapetus Ocean basin. Most models agree that these events occurred at the margin of the palaeocontinent Gondwana, although the precise affiliation (North Africa v Amazonia) is still debated (e.g. Nance and Murphy 1996; Murphy *et al.* 1999; Strachan *et al.* 2007; Linnemann *et al.* 2012). A peri-Baltican affinity for at least some West Avalonian terranes has also been invoked (Landing *et al.* 2022; Beranek *et al.* 2023; Murphy *et al.* 2023).

Previous Neoproterozoic–early Paleozoic terrane maps for southern Britain (e.g. Pharaoh *et al.* 1987; BGS 1996; Pharaoh and Carney 2000) emphasize the presence of tectonic boundaries between terranes with apparently differing magmatic histories and signatures (Fig. 1b). Such maps are strongly influenced by the sampling bias caused by the association of the very limited Precambrian outcrop with major, long-lived tectonic lineaments. Field evidence consistent with terrane displacement is demonstrable along the Llŷn Shear Zone of North Wales (Gibbons 1990; Schofield *et al.* 2008, 2020). Elsewhere, in eastern England and in the Malvern area (e.g. Pharaoh *et al.* 1987), the inferred terrane boundaries are concealed beneath late Paleozoic and/or Mesozoic sedimentary basins. Limited geophysical information is available (Smith 1987; Smith *et al.* 2005) and the nature of these more cryptic terrane boundaries is poorly known. Significant compositional contrasts in latest Ediacaran (570–550 Ma) igneous rocks across the Malvern Lineament (Figs 1, 2) led Pharaoh *et al.* (1987) to infer the presence of distinct Wrekin and Charnwood terranes forming parts of one destructive margin displaced and juxtaposed along the Malvern Lineament. Further lineament-bounded (Cymru and Fenland) terranes were subsequently recognized (Pharaoh and Carney 2000).

Isotopic data (summarized by Schofield *et al.* 2016) and detrital zircon studies indicate that the Precambrian basement of southern Britain south of the Menai Strait and Malvern Lineament resulted from at least three episodes of Cryogenian–Ediacaran subduction magmatism. In a simplification of previous terrane models, we propose that the Fenland, Wrekin and Cymru terranes (Fig. 1b) should be grouped into a newly defined Marches Terrane (Fig. 1c), following the historical name for the Welsh Borderland. This terrane comprises a heterogeneous crystalline complex, including the 711 Ma Stanner–Hanter Complex (Schofield *et al.* 2010) emplaced in the Hanterian Phase at 720–710 Ma, the metaplutonic rocks of the Malvern Hills emplaced at 680–630 Ma during the Malvernian

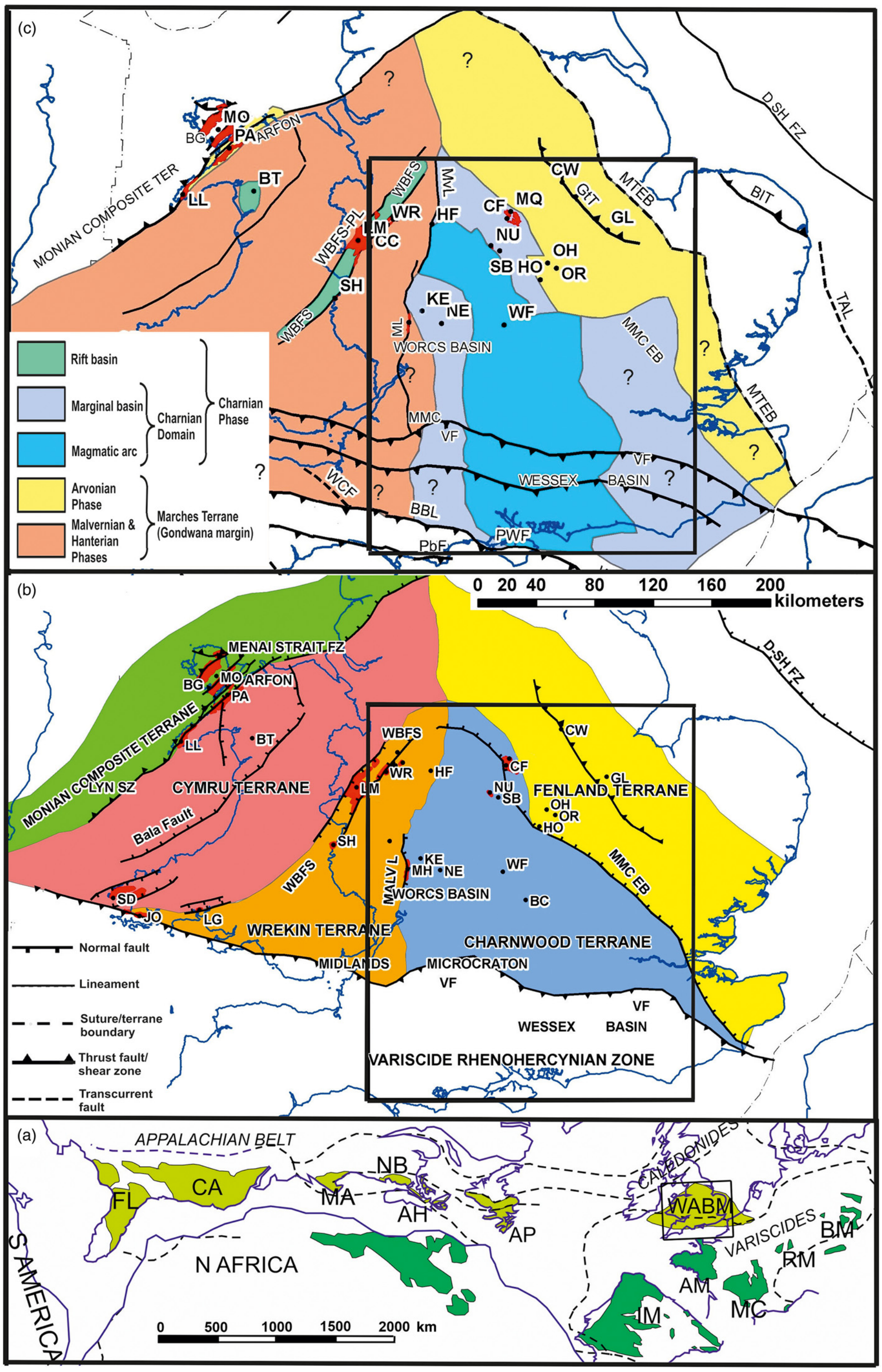

Fig. 1. (**a**) Ediacaran massifs of peri-Gondwanan affinity within the Caledonian–Appalachian–Variscan–Alleghenian orogenic belt. WABM, Wales–Anglo–Brabant Massif (= Caledonide 'East Avalonia Terrane' of Soper *et al.* (1987) coloured olive green); AH, Antigonish Highlands; AP, Avalon Peninsula; CA, Carolinia; FL, Florida; MA, Massachusetts; NB, New Brunswick (= Caledonide 'West Avalonia' terranes coloured light green); AM, Armorican Massif; BM, Bohemian Massif; IM, Iberian Massif; MC, Massif Central; RM, Rhenish Massif (= Variscide 'Cadomian Terranes' coloured dark green). (**b**) Ediacaran terranes in southern Britain. The black rectangle indicates the limit of the area studied in detail. Ediacaran outcrops (highlighted in red): BG, Bwlch-Gwyn (Anglesey) slice; CF, Charnwood Forest; JO, Johnston Complex; LG, Llangynog; LL, Llŷn; LM, Longmynd; MH, Malvern Hills; MO, Monian Composite Terrane; NU, Nuneaton; PA, Padarn; SD, St Davids; SH, Stanner–Hanter Hills; WR, Wrekin. (Latin: Uriconium = The Wrekin). Key boreholes: BT, Bryn-Teg; BC, Bicester 1; CW, Cox's Walk; GL, Glinton 1; HF, Heath Farm 1; HO, Hollowell; KE, Kempsey 1; NE, Netherton 1; OR, Orton; OH, Oxendon Hall; SB, Stretton Baskerville; WF, Withycombe Farm. Significant tectonic structures: D-SH FZ, Dowsing–South Hewett Fault Zone; MMC, Midlands Microcraton; MMC EB, Midlands Microcraton, conjectural eastern boundary; MALV L, Malvern Lineament; VF, Variscan Front; WBFS, Welsh Borderland Fault System. (**c**) Revised map of Ediacaran terranes in southern Britain (this work). The Marches Terrane is considered to occupy all the brown-coloured (Hanterian–Malvernian crust) and yellow-coloured (Arvonian crust) areas. The allochthonous Monian Composite Terrane emplaced in early Ordovician time is not coloured. The Charnian Domain (shades of blue) was injected as a magmatic rift wedge close to the boundary of the Hanterian–Malvernian and Arvonian crust. The black rectangle indicates the limit of the area studied in detail. Question marks indicate areas without deep borehole control and where the identity of the crust is particularly uncertain. Ediacaran outcrops are highlighted in red. Key to outcrop, borehole and tectonic structures as in Figure 1b. Additional significant tectonic structures: 'BBL, Bideford–Bournemouth Lineament; BIT, Broadlands Thrust; CC, Caer Caradoc; GIT, Glinton Thrust; MTEB, Marches Terrane, conjectural eastern limit; LL, Llŷn Shear Zone; ML and MvL, Malvern Lineament; MQ, Morley Quarry No. 1; PbF, Purbeck Fault; PeL, Pendle Lineament; WBFS-PL, Pontesford Lineament; PWF, Purbeck–Wight Fault; TAL, Thames Approaches Lineament; WCF, Watchet–Cothelstone Fault. Source: part (a) modified from Murphy (2007); part (b) after Pharaoh and Carney (2000).

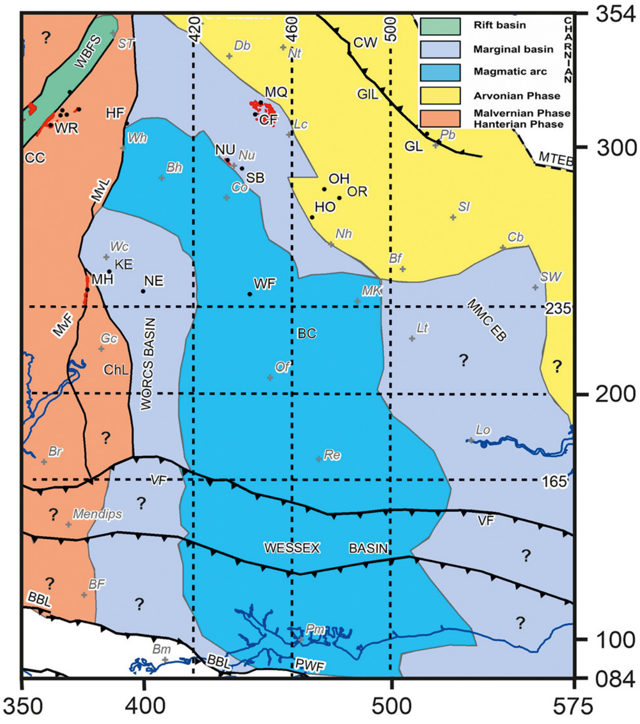

Fig. 2. Boundary of area studied in detail showing the location of Ediacaran outcrop (highlighted in red) and vertical cross-sections through the magnetic susceptibility model (purple dashed lines). Outcrop locality and borehole abbreviations as in legend to Figure 1b. Urban locations: Bf, Bedford; Bh, Birmingham; Br, Bristol; Cb, Cambridge; Co, Coventry; Db, Derby; Gc, Gloucester; Lc, Leicester; Lo, London; Lt, Luton; MK, Milton Keynes; Nh, Northampton; Nt, Nottingham; Nu, Nuneaton; Of, Oxford; Pb, Peterborough; Pm, Portsmouth; Re, Reading; SI, St Ives; ST, Stoke-on-Trent; SW, Saffron Walden; Wc, Worcester; Wh, Wolverhampton.

Phase, as well as metasedimentary protoliths such as the Rushton Schist (Pharaoh and Gibbons 1994). The voluminous eruption of Arvonian welded felsic tuffs from calderas in eastern England at 616–600 Ma was the culminating magmatic event in the formation of this terrane. It is thought to extend beneath the Variscan thrust front to underlie the Mesozoic age Wessex Basin in southern England (Fig. 1c). The previously defined Charnwood Terrane (Fig. 1b) is renamed here the Charnian Domain, comprising volcaniclastic strata (the Charnian Supergroup; Moseley and Ford 1985; Carney 2000*a*) and associated magmatic suites that formed at *c.* 570–550 Ma within that part of the older Marches Terrane lying to the east of the Malvern Lineament.

Aeromagnetic potential field data are particularly useful for identifying the distribution of, and structural trends within, the concealed igneous and metamorphic basement of southern Britain (e.g. Wills 1978; Cornwell and Walker 1989; Lee *et al.* 1991). They allow the continuity of magnetic basement units to be assessed and mapped between limited outcrop and borehole locations. The application of recent inversion modelling techniques (e.g. Beamish *et al.* 2021) can yield further structural detail from historical aeromagnetic datasets and furnishes the basis from which we re-evaluate the extent and nature of the Charnian Domain and its relationship with the surrounding Ediacaran crust. Coeval magmatic suites outwith the Charnian Domain, such as the Uriconian, Llangynog and Bryn-Teg volcanic suites (Fig. 1b, c), are recognized as part of the same phase of magmatism. This approach and the resulting crustal model may find wider application through the Ediacaran terranes shown in Figure 1a.

All grid references in the text refer to the UK National Grid and the height/depth levels (including boreholes) are with respect to the mean sea-level (UK Ordnance) datum (OD) (Z, m). Geophysical data are coordinated in National Grid Easting (NGE = X, km), National Grid Northing (NGN = Y, km) and depth below OD (Z, km).

Review of geological evidence

Charnwood Forest

The most complete exposures of the Charnian Supergroup are the well-known outcrops of Charnwood Forest in the East Midlands of England (Figs 1b, c and 2), which are exposed over an area of *c.* 66 km^2 (Worssam and Old 1988). More than 3.5 km of volcaniclastic strata, with minor reworked epiclastic units, are preserved on either limb of the Charnwood Anticline. Units of matrix-supported volcaniclastic breccia, up to 75 m thick (e.g. the Benscliffe Agglomerate and Sliding Stone Slump Breccia) form marker horizons that facilitate the mapping of an otherwise monotonous succession. These strata represent the immature erosional products of a volcanic arc and were deposited in a tectonically unstable deep-water basin (Moseley and Ford 1985; Wilby *et al.* 2011).

Penecontemporaneous andesitic and dacitic lava domes and their marginal screens (Carney 2000*b*) are interbedded with the volcaniclastic strata. The latter have been intensively studied because they contain the impressions of a diverse metazoan biota of Ediacaran age (Boynton 1978; Liu *et al.* 2015; Kenchington *et al.* 2018), including the iconic organism *Charnia* (Ford 1958) and *Auroralumina attenboroughii*, recently recognized as a true animal (Dunn *et al.* 2021). The Charnian Supergroup is intruded by microdiorite dykes (the North Charnwood Diorite Suite) and larger bodies of granophyric diorite (the South Charnwood Diorite Suite). Geochemical studies have demonstrated that the intrusive rocks and the volcaniclastic strata are genetically related, forming parts of one magmatic series (Pharaoh *et al.* 1987). Detrital zircon grains from the oldest exposed strata (Blackbrook Group) have been dated at 569.1 ± 0.9 Ma or older and zircon grains from the overlying Maplewell Group at 561.9 ± 0.9 to *c.* 557 Ma (zircon U–Pb; thermal ionization mass spectrometry) constrain the maximum depositional age (Noble *et al.* 2015).

Nuneaton quarries

The only other significant outcrop of the Charnian Supergroup occurs near Nuneaton (Figs 1b, c and 2), where the correlative Caldecote Volcanic Formation (Allen 1968; Bridge *et al.* 1998) occupies a small (*c.* 2.8 km^2) inlier. A thick (>100 m) unit of massive, coarse-grained, crystal, crystal–lithic and lapilli tuffs of mainly dacitic composition contains large (metre-scale) rafts of finer grained bedded tuff. The unit is petrographically similar to the volcaniclastic breccia units in Charnwood Forest, but exhibits less matrix support. Similar rocks were encountered in Stretton Baskerville borehole [SP 400 912] (Fig. 2). A north–south-striking suite of microdiorite dykes up to 50 m wide is geochemically indistinguishable from the North Charnwood diorites and locally coincident with Precambrian faults (Bridge *et al.* 1998). A stock of granophyric diorite (Wills and Shotton 1934) geochemically identical to the South Charnwood diorite has yielded a U–Pb zircon age of 603 ± 2 Ma, interpreted as the age of crystallization (Tucker and Pharaoh 1991) This interpretation has to be reconsidered because the Charnian Supergroup (which the granophyric diorites intrude) ranges in age from 569 to *c.* 557 Ma (Noble *et al.* 2015) and the 603 Ma zircon grains are likely to be xenocrystic.

Malvern Hills

The Malvern Hills largely comprise the Malvern Plutonic Complex (MPC), a diverse calc-alkaline plutonic suite emplaced at *c.* 680 Ma and subsequently affected by garnet–amphibolite metamorphism, heterogeneous ductile shearing at *c.* 650 Ma, mylonitization and the injection of pegmatites at *c.* 610 Ma (Strachan *et al.* 1996). The Warren House Formation crops out in a small area (*c.* 0.5 km^2) at Broad Down [SJ 765 395], in inferred tectonic contact with the MPC. The formation comprises interbedded spilitic basalt lavas, locally pillowed, altered intermediate to silicic lavas and welded tuff, and is much less deformed and metamorphosed than the Malvern Plutonic Complex (MPC) with which they are juxtaposed along the Malvern Lineament (Beckinsale *et al.* 1986). Intrusion of the MPC at *c.* 680 Ma (Tucker and Pharaoh 1991) was followed by garnet–amphibolite metamorphism, pegmatite injection, and heterogenous ductile shearing (Strachan *et al.* 1996). Undeformed rhyolitic tuff from yielded a U–Pb zircon age of 566 ± 2 Ma, interpreted as the age of eruption (Tucker and Pharaoh 1991). North–south-striking dykes of dolerite and microdiorite cross-cutting the ductile fabrics and late pegmatites of the MPC are also inferred to be of Ediacaran age.

Wrekin area

Uriconian volcanic rocks outcrop within and around the Welsh Borderland Fault System (WBFS; Woodcock and Gibbons 1988) (Figs 1, 2). Up to 2000 m of subaerially erupted basaltic andesite, andesite, dacite and rhyolitic lavas, and tuffs are present in the various fault-bounded outcrops (e.g. at Caer Caradoc and the Wrekin) (Fig. 2). A felsic welded tuff yielded a U–Pb zircon age of 565 ± 2 Ma (Tucker and Pharaoh 1991). The Longmyndian Supergroup, apparently overlying the Uriconian lavas, comprises *c.* 8 km of green, grey and purple mudstone, flaggy siltstone and turbiditic sandstone. The basal Stretton Group was deposited in deeper water than the overlying Wentnor Group, which contains abundant shallow water sedimentary structures. Zircons from thin units of airfall tuff and ash in the Stretton Group yielded U–Pb ages of 566.6 ± 2.9 Ma and 555.9 ± 3.5 Ma (Compston *et al.* 2002). The succession is folded into an overturned isoclinal syncline, which is presumed to predate Cambrian deposition (Greig *et al.* 1968). The Longmynd Syncline can be interpreted as a deformed rift basin, with the Uriconian lavas occupying positive flower structures between strands of the WBFS and the Longmyndian forming a tightly compressed (inverted) rift-fill succession.

Borehole evidence

Six boreholes penetrate inferred Charnian rocks, some concealed by younger cover (Pharaoh and Gibbons 1994). As a result of the small amount of core recovered, the interpretation of geophysical logging suites contributes significantly to the lithological interpretation and a table of petrophysical data is included in Supplementary Publication 1. Morley Quarry No. 1 borehole [SK 4765 1787] was drilled within Charnian outcrop (Fig. 2) and in its upper (uncored) part penetrated massive breccia, tuff and lithic sandstone, developed in at least two sharply based, fining-up depositional cycles (Pharaoh and Evans 1987). Beneath 410 m OD, a massive unit of porphyritic dacite is compositionally similar to the dacite lavas in the exposed succession. Sonic log values range up to 6000 m s^{-1} in the basal dacite unit (Supplementary Publication Table 1). Log densities range from 2.67–2.69 Mg m^{-3} in the tuffs to 2.69 Mg m^{-3} in the basal dacite.

The continuously cored Withycombe Farm borehole [SP 4319 4017], located *c.* 75 km south of Charnwood (Fig. 2), was drilled on the Banbury magnetic anomaly in Oxfordshire (Poole 1978). Thirty metres of dark grey–green basaltic andesite and light grey dacite lava, locally vesicular and brecciated, are overlain by early Cambrian sandstones (Rushton and Molyneux 1990). Very high magnetic susceptibility values (0.063 SI units) are encountered in the basaltic andesite lavas towards terminal depth (TD), which are denser (2.78–2.90 Mg m^{-3}) and exhibit a higher sonic velocity (6189 m s^{-1}) than any other Charnian suite, except for the North Charnwood diorites (Supplementary Publication Table 1). The Cambrian sandstones exhibit moderate magnetic susceptibility (0.014 SI units) attributed to a high magnetite content (about 2%; Poole 1978) and potentially contribute to the Banbury magnetic anomaly (Busby *et al.* 2006).

Heath Farm 1 borehole [SJ 9333 0926] lies close to the northward prolongation of the Malvern Lineament (Fig. 2). The Shell company log infers a volcano-sedimentary succession underlying early Cambrian (Wrekin) quartzite at 1565 m below OD. Forty-one metres of red–brown siltstone and sandstone (cf. Longmyndian strata) overlie 137 m of mottled red, green, brown and white feldspathic agglomerate and tuff. The deepest core penetrated green–grey laminated tuff and agglomerate, with 0.2–2 m thick pink, orange and red fine-grained silicic bands. Distortions of bedding by slumping, volcanic bombs, pumice and black glassy welded intervals are described in the borehole log. The presence of possible Longmyndian strata overlying the volcanic rocks favoured their lithological correlation with the Uriconian succession in outcrop (Pharaoh and Gibbons 1994). The sonic velocity and density values are lower than those at the Netherton 1 and Kempsey 1 boreholes and may reflect penecontemporaneous weathering.

The uncored Netherton 1 borehole [SO 9982 4138] (Fig. 2) penetrated 560 m of felsic tuff beneath 1709 m of Jurassic, Triassic and Permian strata. Two sidewall cores at 1809 and 2236 m below OD comprised grey–green graded and non-welded, vitric–lithic tuff. A K–Ar whole-rock age of 424 ± 8 Ma (Silurian) reported by Harrison (1974) is here considered unreliable. Pyroclastic grains include argillized glass shards and pumice and microlitic basalt. These rock types bear a strong resemblance to those encountered in the Heath Farm 1 borehole. The Netherton 1 gamma log contains very clear evidence of cyclicity, showing up to six sharply based massive units, typically 40 m or more thick, interpreted by us as debris flow breccias, passing up into thin, better-layered units, here interpreted as 'background' volcaniclastic airfall. The sonic velocity is identical (within error) to that in the nearby Kempsey 1 borehole, at 5501 and 5569 m s^{-1}, respectively (Supplementary Publication Table 1), significantly exceeding that of the Silurian volcanic rocks (Kearey and Rabae 1993) in the Bicester 1 borehole (Fig. 1b).

The Kempsey 1 borehole [SO 8609 4933], drilled to 2985 m below OD (Fig. 2), penetrated 706 m of grey–green and mottled brown volcaniclastic rocks beneath 2305 m of Permo-Triassic strata (Whittaker 1980; Whittaker *et al.* 1985). Three short cores sampled agglomerate and tuff with poorly sorted angular to subrounded clasts of trachyandesite and rhyolite lava, reworked welded, crystal and vitric tuff, and red, brown, purple and green tuffaceous sandstone (Barclay *et al.* 1997). The latter exhibit fining-upwards grading, cross-bedding and erosive channel features. Two major fining-upwards cyclic units up to 150 m thick are comparable in scale with those in the Morley Quarry borehole, but are not as clearly expressed as at the Netherton 1 borehole. The basal massive agglomeratic part of each cycle, typically 10–20 m thick, with gamma values <50 API units and a slightly greater density (up to 2.75 Mg m^{-3}) is overlain by a unit interpreted as bedded volcaniclastic tuff and sandstone.

Eastern boundary of the Charnian Domain

A few boreholes help to define the approximate position of the concealed eastern boundary of the Charnian Domain (Fig. 2). Historical (nineteenth century) water bores at Orton and Oxendon Hall (Figs 1, 2) encountered felsic volcanic rocks (Dearnley 1966) with an enriched geochemical and isotopic signature distinct from the depleted signature typical of the Charnian magmatic rocks

(Pharaoh *et al.* 1991; Noble *et al.* 1993; Pharaoh and Gibbons 1994). The welded felsic tuff intersected by the Glinton 1 borehole is petrographically identical to the Orton occurrence (Dearnley 1966) and both have yielded U–Pb zircon ages in the range 616–612 Ma and T_{DM} model ages in the range 1650–1400 Ma (Noble *et al.* 1993), comparable with those of Arvonian felsic volcanic rocks in North Wales (Reedman *et al.* 1984; Tucker and Pharaoh 1991; Schofield *et al.* 2016). The Hollowell borehole [SP 6833 7183] (Figs 1, 2) intersected 24 m of green, purple and brown agglomeratic breccia and bedded tuff beneath Triassic basal breccia (Allsop *et al.* 1987). The agglomerate fragments comprise intermediate to felsic volcanic rocks (e.g. microlitic amygdaloidal and microphyric lava, flow-banded trachytic lava and perlitic rhyolite) with a geochemical composition similar to that of the Arvonian volcanic rocks described earlier (Pharaoh *et al.* 1991). Sonic and density log values are comparable with the boreholes described in Supplementary Publication Table 1. However, most of the debris in the overlying Triassic breccia has a Charnian provenance (Pharaoh *et al.* 1991).

Magnetic anomalies in southern Britain: study area and previous investigations

The main part of this study comprises the modelling and 3D inversion of aeromagnetic data within the 270 km (Y) by 225 km (X) (60 750 km^2) region of central and southern Britain shown in Figures 2 and 3. The terminology for the magnetic anomalies shown in Figure 3 and elsewhere uses a scheme developed from Busby *et al.* (2006) and is superimposed on the reduced-to-pole aeromagnetic dataset.

This region is known to contain several Paleozoic magmatic suites, both at outcrop and subcrop, in addition to the Ediacaran rocks that are the focus of this study. The South Leicester Diorite Complex (MA08) and the Mountsorrel Granodiorite (Le Bas 1972), emplaced at *c.* 452 Ma in the late Ordovician (Noble *et al.* 1993), are associated with the western part of the Derby–St Ives Magnetic Anomaly (Fig. 3) (Cornwell and Walker 1989). Further bodies of diorite and granodiorite are encountered by boreholes farther east (MA03, MA09 and MA10). MA13 and MA14 form part of the Furness–Ingleborough–Norfolk Magnetic Anomaly (Fig. 3), for which various potential Caledonian magnetic sources have been invoked (Chroston *et al.* 1987; Lee *et al.* 1991). Early Silurian lavas crop out in Somerset and Gloucestershire (MA37; Fig. 3) and were penetrated by the Bicester 1 borehole (Kearey and Rabae 1993; Cornwell *et al.* 1994) in Oxfordshire (Fig. 1b). Late Carboniferous magmatic rocks are associated with the Oxfordshire–Berkshire (MA26W) and Nottinghamshire (MA02–MA05) coalfields (Ellis and Kearey 1984; Horton *et al.* 1987; Foster *et al.* 1989; Kearey 1991). As far as is known, no intrusion from the Paleocene North Atlantic suite is present in the area.

Most of the study area is dominated by an SSE-trending complex magnetic high (MA22–MA 27) *c.* 190 km long by 40–80 km wide (Fig. 3), forming the South-Central England Magnetic Anomaly (SCEMA) of Kearey (1991) or the Magnetic Ridge 3 of Wills (1978). Kearey (1991) invoked a deep Carboniferous basaltic source for the SCEMA within the mid-crust and such bodies may indeed contribute – for example, in the Reading area (Fig. 2), the Withycombe Farm borehole is located on one of the individual highs (Figs 1–3) and penetrated Precambrian lavas with a moderately high magnetic susceptibility of 0.063 SI units (Poole *et al.* 1978). Lee *et al.* (1991) and Pharaoh *et al.* (1991) speculated that the SCEMA represents the plutonic core of a Charnian magmatic arc within the Midlands Microcraton. The magnetic domain is segmented by WSW-trending magnetic and gravity lineaments. One just south of the Withycombe Farm borehole apparently causes a sinistral offset of the SCEMA (Lee *et al.* 1991; Busby and Smith

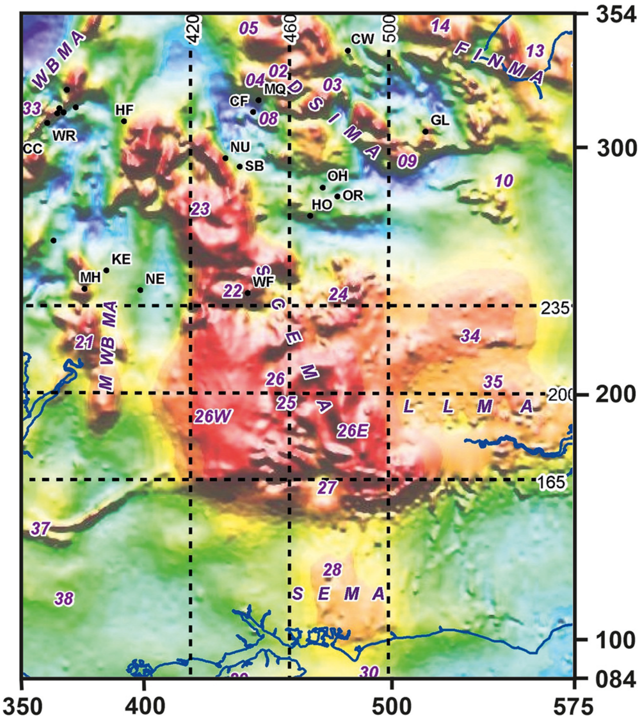

Fig. 3. Aeromagnetic map of the area of detailed study, showing the limits of the magnetic susceptibility model and location of selected vertical sections (dashed lines). The base map comprises reduced-to-the-pole, total magnetic field data displayed as a colour-shaded relief map, illuminated from the north (following Busby and Smith 2001). The key to abbreviated names for Ediacaran outcrop and key borehole locations (black points) is given in the legend to Figure 1. Abbreviated names of previously identified magnetic anomaly (MA) complexes described in the text: DSIMA, Derby–St Ives MA; FINMA, Furness–Ingleborough–Norfolk MA; LLMA, London–Luton MA; MWBMA, Malvern–Worcester Basin MA; SCEMA, South Central England MA; SEMA, Southern England MA; WBMA, Welsh Borderland MA. Abbreviated codes for magnetic anomalies (following Busby *et al.* 2006): 02, Widmerpool MA; 03, Melton Mowbray MA; 04, Derby MA; 05, Nottingham MA; 08, South Leicestershire MA; 09, Rutland MA; 10, Warboys MA; 13, South Wash MA; 14, FINMA; 21, Malvern MA; 22, Banbury MA; 23, Birmingham MA; 24, Milton Keynes MA; 25, Oxford MA; 26, SCEMA; 27, Reading MA; 28, SEMA; 31, Central Channel MA; 33, WBMA; 34, Luton MA; 35, London MA; 37, Mendip Hills MA; 38, Blandford MA.

2001) and divides the SCEMA into a relatively narrow (30 km wide) northern part and a broader (80 km) and more complex southern part. MA34 in the Luton area has previously been interpreted as a block of relatively magnetic basement within the microcraton (Cornwell and Walker 1989), although it is discordant to the previously proposed NW-trending eastern boundary of the microcraton (e.g. Lee *et al.* 1991; Molyneux 1991; Woodcock 1991).

A complex set of anomalies (MA33) is associated with the outcrop of Uriconian mafic lavas and tuffs around the WBFS (Figs 1b, c and 3). The individual peaks of the magnetic anomaly contrast with a background of weakly magnetic basement, which extends to the Malvern Lineament (Fig. 3). In the Worcester Basin, MA21 (Magnetic Ridge 4 of Wills 1978) is spatially linked to surface outcrops in the Malvern Hills. The aeromagnetic and gravity anomalies in this region were modelled along a west–east profile across the Worcester Basin by Barclay *et al.* (1997, their fig. 45). In this model, 'weakly magnetic basement' with a modelled magnetic susceptibility (MMS) of 0.0012 SI units and a density of 2.70 Mg m^{-3} is interpreted as the source of the low-amplitude MA21 associated with the upthrust diorite–granodiorite of the MPC and is also inferred to underlie the western part of the Worcester Basin.

3D inverse modelling of regional magnetic potential field data

Methods

The baseline aeromagnetic data used in the modelling described here were acquired between 1955 and 1965. The flying height within the study area was largely between 457 and 549 m (mean 503 m) and the flight line spacing was 2 km. The inversion method (MAG3D) used here was originally developed by Li and Oldenburg (1996). The algorithm assumes that the measured magnetic field is generated by induced magnetization alone and a positivity constraint is applied to the susceptibility, which is thus constrained to be greater than zero. The value derived from the modelling is referred to as the MMS to distinguish it from observed magnetic susceptibility. This procedure recovers a spatially smooth representation of the subsurface structure (Beamish *et al.* 2021).

In the present work, the data grid cell size used is 1 $(X) \times 1$ (Y) km with a depth (Z) scale of 1 km, generating a voxel dataset with the same dimensions. The data were continued upward to a height of 1 km. As discussed by Beamish *et al.* (2021), the Curie temperature isotherm corresponds to the basal surface of any magnetic crustal model. The inversion procedure, by itself, is unable to establish the crustal magnetic depth. Curie depth estimates across onshore Britain (Baykiev *et al.* 2018, their fig. 9b), ranging from 27.5 km (western Scotland) to 32.5 km (southern England), are significantly shallower than the estimated Moho depth (≤40 km), particularly in the study area (Baykiev *et al.* 2018, their fig. 9c). Our 3D model assigns a magnetic depth of 32 km below OD.

Crustal depth is the only defined geological parameter in an otherwise unconstrained inversion (Lelièvre *et al.* 2009). Beamish *et al.* (2021) demonstrated that a crustal swathe model of Britain obtained by 3D inversion yielded good agreement with a previous geologically constrained 2.5D profile inversion across northern Britain. The core area of the model contains 270 × 225 × 32 voxel cells and is covered by 61 246 observations. The model presented uses depth weighting with smoothing across distance scales of 4 km × 4 km × 2 km. For the purposes of display, values <0.001 SI units are regarded as effectively non-magnetic. The misfit of the model presented here has a standard deviation of only 3.0 nT with a 95% interquartile of 6.9 nT. The predicted data of the 3D inversion therefore fit the observations with a high degree of fidelity at all wavelengths. The maximum value of the MMS returned by the inversion is 0.07 SI units. The MMS data were built into a 3D petrophysical model using PETREL (® Schlumberger) seismic interpretation software, from which a series of visualizations was extracted.

Visualization and interpretation

The 3D inversion model can be visualized by slicing in the direction of the X, Y and Z axes. Figure 4 presents the modelled data as horizontal slices (maps) at selected depth (Z values) across the entire area of study. Vertical cross-sections with no vertical exaggeration are presented in Figures 5 and 6. Another way to view the MMS dataset is to produce depth–structure maps in which the deep structure of the model at a particular magnitude of MMS can be

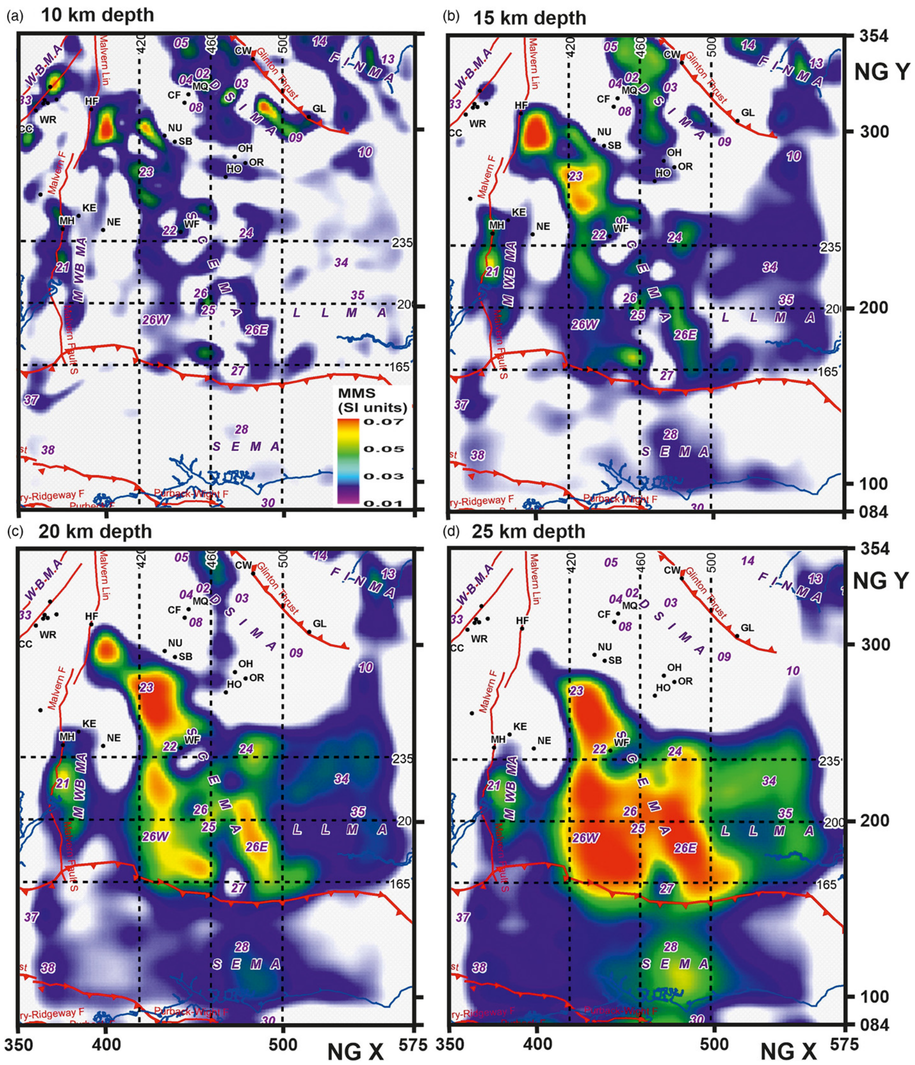

Fig. 4. Depth slice maps through the magnetic susceptibility model showing the modelled magnetic susceptibility (MMS) values at depths (Z values) of (**a**) 10 km, (**b**) 15 km, (**c**) 20 km and (**d**) 25 km. For key to abbreviations, see legend to Figures 1 and 3.

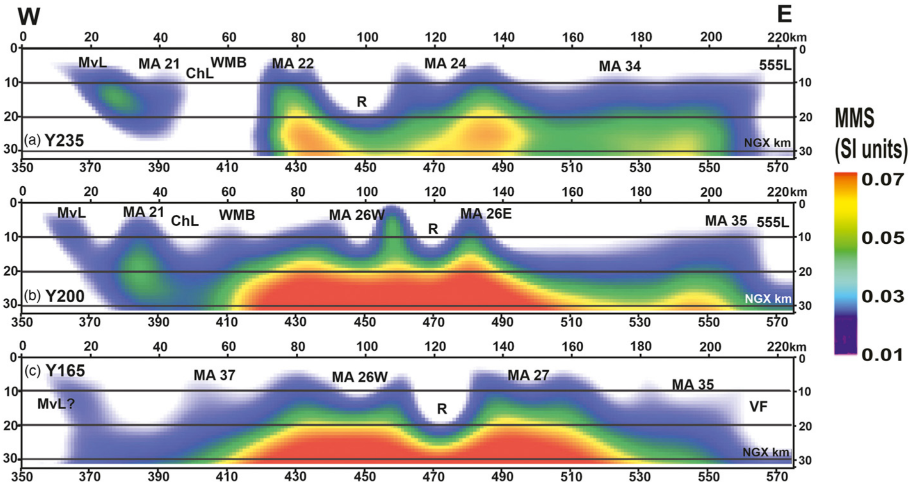

Fig. 5. West–east-oriented vertical cross-sections, showing the modelled magnetic susceptibility (MMS) values along profiles at National Grid Y (m) values of (**a**) 235 000, (**b**) 200 000 and (**c**) 165 000. The locations of the sections are shown on Figures 2 and 4. In each case, the lower scale is in terms of National Grid *X* (km) values and the upper scale is in terms of kilometres from the origin (in the west). For key to abbreviations of tectonic elements and magnetic anomalies, see the legends of Figures 1 and 3. Additional inferred elements: R, intra-arc rift; WMB, Worcester (back-arc) marginal basin.

examined (Fig. 7). The depth-contoured values are created by setting a threshold within the MMS dataset across a narrow range of MMS values. This enables lineaments and other structural detail within the model to be more easily recognized and mapped. These features are mapped on Figure 7, but, for clarity, are labelled on the synoptic interpretation diagram (Fig. 8). 3D perspective models further aiding visualization can also be readily generated from the 3D model. Unannotated versions of Figures 4–7 are provided in Supplementary Publication 1; see Busby *et al.* (2006) for a further description of the magnetic anomalies attributed to the post-Ediacaran sources in the previous section. These will not be discussed further here.

South-Central England Magnetic Anomaly

The SCEMA is the only component of the model that apparently extends through almost the entire crust from 5 to 32 km depth (Figs 4–6). Its surface is shallowest in the north at *c.* 5 km depth and deepens to *c.* 8 km just to the north of the Variscan Front (Fig. 6a). The western edge of MA23 is sharply delimited by faults forming the NE edge of the Warwickshire Coalfield. Segmentation of the belt (MA22–MA23 from MA24–MA26) is associated with west–east-trending lineaments, especially at 250L (Figs 7, 8). The SCEMA is much wider and more complex south of 250L (Fig. 7) and exhibits higher MMS values there, particularly at greater depths (Fig. 4). MA26, which forms the major part of the SCEMA, exhibits considerable internal complexity. It is terminated rather sharply to the east by an NNW-trending lineament, bounding MA24 and MA26E, and separating it from MA34–MA35. On the western and eastern flanks of MA26, the upper surface of the source appears smooth and planar (MA26W, Fig. 6a and MA26E, Fig. 6c), but several looping and ring-like magnetic features up to 40 km in diameter dominate the anomaly pattern at 10–15 km depth in the core of MA26 (Figs 4a, 4b, 7a, 8) to the north and south of Oxford. Some of these annular features reach to within 2–3 km of the surface (e.g. near the Withycombe Farm borehole, MA22; Figs 5a, 6a). At 20 km depth (Fig. 4c), MA26 is more homogeneous, except for an NNW-trending rift-like structure that bifurcates the anomaly (Figs 5a–c, 6b, 8) and upon which the annular structures appear superimposed. In Figure 7d (MMS values >0.035 SI), MA23 is much smaller in area than at shallower crustal levels.

South England Magnetic Anomaly

Although the expression of the South England Magnetic Anomaly (SEMA) is muted by the superimposed late Paleozoic and Mesozoic strata of the Wessex Basin at shallow (<10 km) depths (Fig. 3a), it is clear that the SEMA represents the continuation of the SCEMA to the south at greater (>15 km) depths (Figs 4c, 6). Segments of MA28 may be dextrally offset from MA26–MA27 south of the Variscan Front on the Wiltshire Lineament, as well as on lineaments farther south (the North Hampshire Lineament–South Sussex Lineament) (Figs 7b, c and 8). The cross-sections confirm that the surface of MA28 is flat in the west, lying at *c.* 14 km depth (Fig. 6a–c). The vertical offset from the SCEMA to the SEMA, *c.* 20 km to the south of the mapped shallow crustal position of the Variscan Front (Fig. 7c, d), is of the order of 4–5 km and the boundary has an apparent dip to the south of 20°.

London–Luton Magnetic Anomaly

The London–Luton Magnetic Anomaly forms a distinct shelf-like feature projecting eastward from MA26. It is barely discernible at

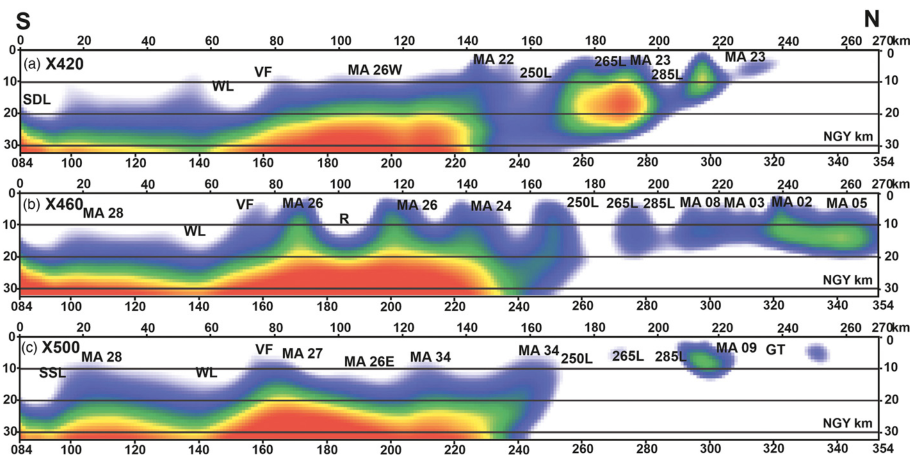

Fig. 6. South–north-oriented vertical cross-sections showing the modelled magnetic susceptibility (MMS) values along profiles at National Grid *X* (m) values of (**a**) 420 000, (**b**) 460 000 and (**c**) 500 000. Same colour scale as Figure 5. The locations of the sections are shown on Figures 2–4. In each case, the lower scale is in terms of National Grid *Y* (km) values; the upper scale is in terms of kilometres from the origin (in the south). For key to abbreviations of tectonic elements and magnetic anomalies, see the legends of Figures 1–3. Additional inferred elements: R, intra-arc rift; WMB, Worcester (back-arc) marginal basin.

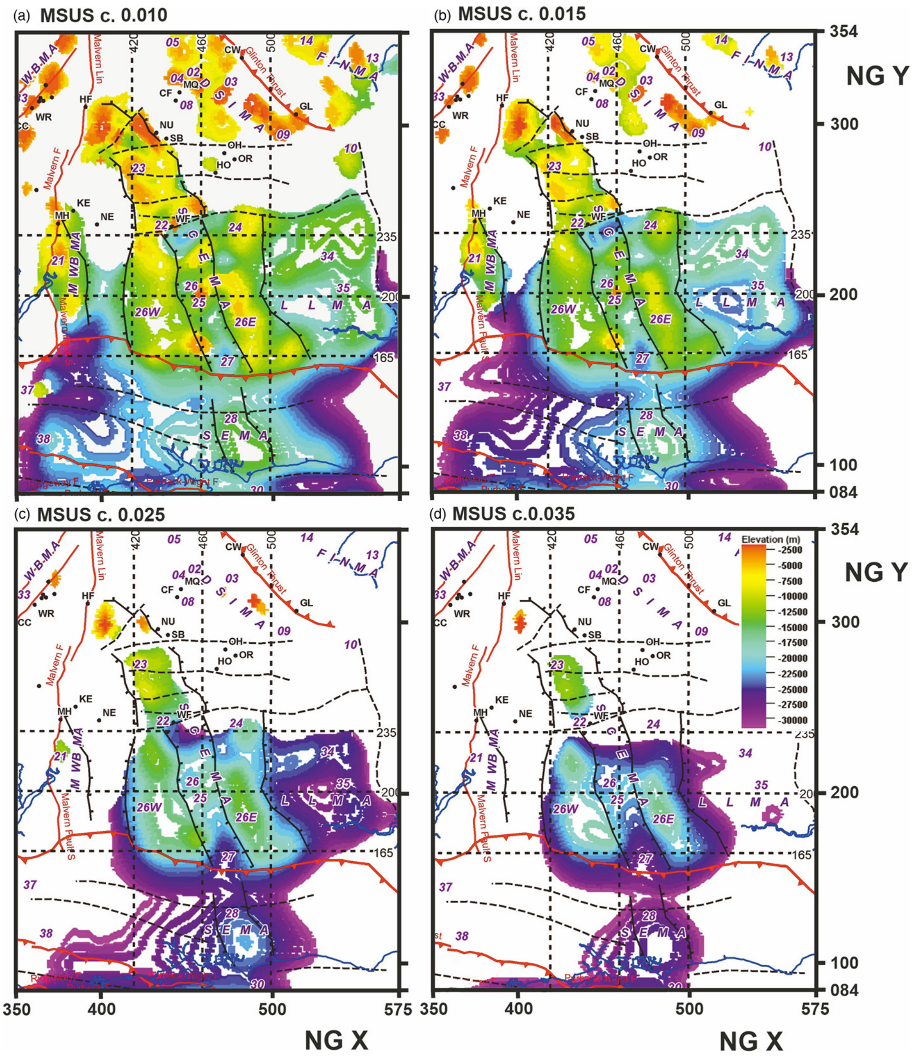

Fig. 7. Depth–structure maps of the area of detailed study derived by thresholding the modelled magnetic susceptibility values showing depth (in metres) to the top of surfaces with modelled magnetic susceptibility values of (**a**) *c.* 0.010, (**b**) 0.015, (**c**) 0.025 and (**d**) 0.035 SI units. The decreasing density of data points with increasing depth results in more discrete contouring in the south of the study area. Inferred deep structural lineaments within the model are mapped, but not labelled for clarity.

10 km depth (Fig. 4a), but strengthens significantly at 20–25 km depth, where it appears distinct from MA26. Figure 7d suggests that the highest MMS values (>0.035 SI units) exhibited by MA26 are not shown by MA34 and MA35. The eastern limit of the anomaly is the north-trending Saffron Walden Lineament (555L) (Figs 7b, 8), which has steep to vertical dips throughout its length (Fig. 5).

Malvern–Worcester Basin Magnetic Anomaly

This anomaly is associated with the surface outcrop of the MPC (Fig. 3), but also extends east of the Malvern Lineament to include the western part of the Worcester Basin (Fig. 4b–d) below 15 km depth (Cornwell 1992). The Cheltenham Lineament forms the eastern edge of the Malvern–Worcester Basin Magnetic Anomaly at <15 km depth (Fig. 5a, b). MA21 merges with MA26W (the SCEMA) below 15 km depth (Fig. 4b). Only a very small part of the magnetic anomaly exhibits MMS >0.025 SI units, unlike the SCEMA. MA38 is likely to be a continuation of MA21 (and the MPC) into the mid-crust south of the Variscan Front.

Welsh Borderland Magnetic Anomaly

The crust west of the Malvern Lineament is significantly less magnetic than the crust to the east. The Welsh Borderland Magnetic Anomaly consists of a scatter of smaller anomalies, particularly concentrated in and around the WBFS and at shallow crustal (<10 km) depth (Fig. 4a, b). The MMS values are mostly <0.015 SI units.

Source of the long-wavelength magnetic anomalies in the mid- and lower crust

Kearey (1991) proposed that the source of the SCEMA was a large Carboniferous body of basic or ultrabasic composition, emplaced into the mid-crust during a phase of pre-Variscan subduction. The absence of a strong positive gravity anomaly is problematic (Kearey 1991) unless the body has a density more comparable with the bulk crust (i.e. *c.* 2.75 Mg m^{-3}). It is proposed here that ferromagnesian cumulate units of mafic–intermediate compositions (gabbro, diorite and granodiorite), akin to the exposed MPC (Barclay *et al.* 1997), may be a more plausible source. MA26, at the core of the SCEMA, is coincident with the deepest Moho (*c.* 36–40 km) in the UK (Baykiev *et al.* 2018; Licciardi *et al.* 2020). Potentially, there may also be a local contribution from magnetite-rich Cambrian strata and from Silurian volcanic rocks (Kearey and Rabae 1993; Cornwell *et al.* 1994). In general, these other Paleozoic potential sources are areally and volumetrically restricted, lie within thin (<200 m) stratigraphic/intrusive units and are predicted to generate short-wavelength anomalies (Busby and Smith 2001). Neoproterozoic magmatic units are potentially more widely distributed, are presumed to occupy the greater part of the depth of the crust and are therefore considered to make the most significant contribution to the long-wavelength magnetic anomalies of the SCEMA.

A fuller understanding of the possible sources of the magnetic anomalies described here can be achieved by mineralogical, geochemical and petrogenetic investigations of the Neoproterozoic magmatic rocks. This is despite the limited number of samples

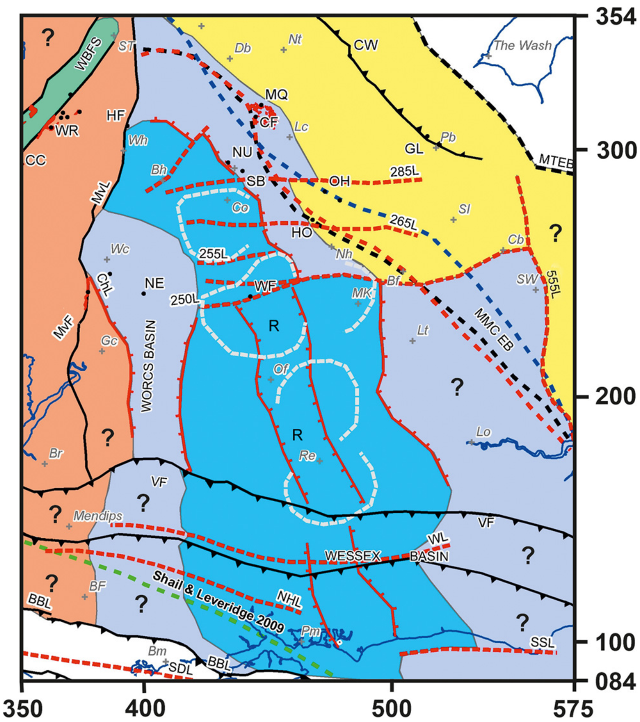

Fig. 8. Synoptic interpretation map of crustal structure in the study area. Ediacaran crustal structure derived from an interpretation of Figures 4 and 7: red, inferred extensional faults (ticks) and late lineaments (dashed); R, Median Rift; white dashed line, inferred caldera structures. Lineaments mapped on Figure 7 are labelled. 250L, Bedford Lineament; 255L, unnamed; 265L, unnamed; 285L, Coventry Lineament; 555L, Saffron Walden Lineament; BBL, Bideford–Bournemouth Lineament; ChL, Cheltenham Lineament; NHL, North Hampshire Lineament; SDL, South Dorset Lineament; SSL, South Sussex Lineament; WL, Wiltshire Lineament. Caledonian and Variscan upper crustal structure: black, thrusts (with ticks) and extensional faults. For key to colours, and urban locations, see legend to Figure 2. Thick dashed lines show the inferred location of concealed putative structural elements: dark green, MMCEB after Lee *et al.* (1991); red, MMCEB after Molyneux (1991); blue, MMCEB after Woodcock (1991); light green, Wight–Bristol Channel Fault after Shail and Leveridge (2009).

available from surface outcrops and boreholes, which typically sample only the uppermost few kilometres of the crust.

Petrogenesis of the Charnian magmatic rocks

Representative geochemical data for magmatic suites attributed to the 570–550 Ma Charnian magmatic phase in central and southern England are shown in Figures 9 and 10. Both new (e.g. the deep boreholes reviewed earlier and Longmyndian surface outcrops) and previously published data are included. The analytical methods and data are listed in Supplementary Publication 2.

The majority of the Charnian igneous rocks are not severely deformed. Regional metamorphism in the zeolite and greenschist facies is pervasive, however, so that little, if any, of the primary mineralogy is preserved. Ferromagnesian minerals are pseudomorphed by chlorite and epidote. Calcic plagioclase is altered to more sodic varieties. These observations are consistent with mobility of the major elements (Si, Ca, K and Na) and other large ion lithophile elements (LILEs). Loss-on-ignition values demonstrate variable hydration and carbonation. Consequently, a greater emphasis is placed on the content of high field strength elements (HFSEs), which are less mobile (Pearce 1982; Pharaoh *et al.* 1987). Data gaps are interpolated using suitable proxy elements (e.g. Nb for Ta) where key elemental data are missing.

Mafic magmas of the Charnian phase include basalt and basaltic andesite lavas from Charnwood and the Withycombe Farm borehole (Fig. 9a) and the Warren House Formation of the Malvern Hills (Fig. 9c), all exhibiting flat geochemical patterns for the HFSEs (Ta to Yb), close to those of mid-ocean ridge basalt (MORB). The chondrite-normalized rare earth element patterns for the Warren House Formation are flat (Fig. 10c), but other components show slight light rare earth element enrichment (Fig. 10a, b, d). Slight enrichment of Ce and Th with respect to Nb (and Ta where analysed) is comparable with that of island arc tholeiite magmas with a supra-subduction component from marginal basins in the western Pacific (e.g. Saunders and Tarney 1984). Slightly greater enrichment of Ce and Th is observed in undeformed Malvern dolerite and microdiorite dykes (Fig. 9c) and Uriconian basaltic andesites (Fig. 9d). The Withycombe Farm borehole dacite and Charnian eruptive dome-forming andesite

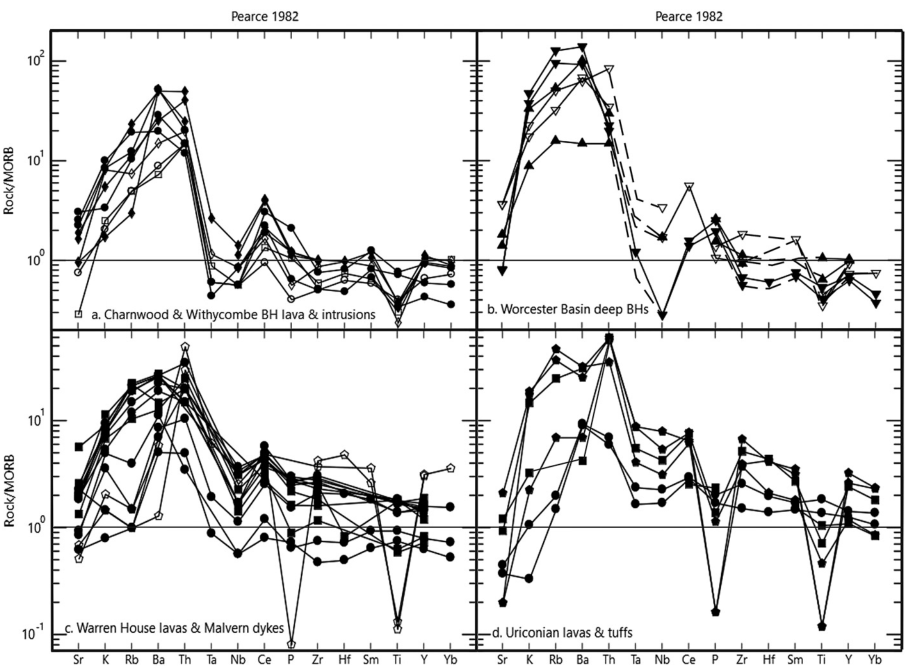

Fig. 9. MORB-normalized geochemical variation diagrams for components of the Charnian magmatic phase. MORB-normalization factors after Pearce (1982). Data from Pharaoh *et al.* (1987) except where indicated. (**a**) Charnwood Forest, Nuneaton and Withycombe Farm borehole (previously unpublished). (**b**) Volcaniclastic rocks from Worcester Basin boreholes. Data from Barclay *et al.* (1997) and previously unpublished data. (**c**) Warren House formation lavas and mafic dykes from the Malvern Hills (Thorpe 1974). (**d**) Uriconian lava and tuff from the Wrekin and Caer Caradoc areas. Circles, basaltic andesite lava and microdiorite; squares, andesite lava; diamonds, dacite lava; pentagons, rhyolite lava; triangles, felsic tuff and ash.

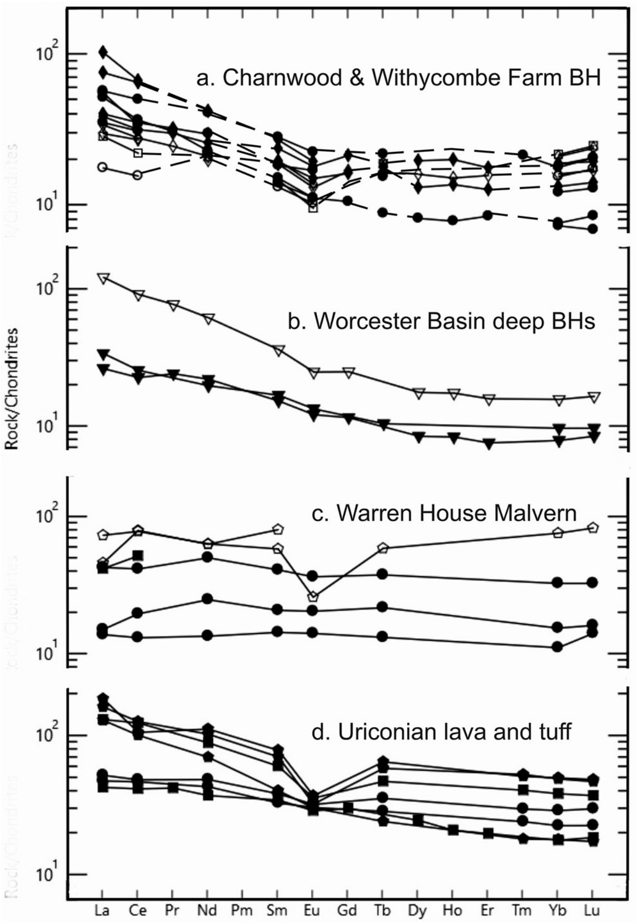

Fig. 10. Chondrite-normalized rare earth element patterns for the same components of the Charnian magmatic phase as in Figure 9. Key to symbols are in legend to Figure 9.

(Fig. 9a) exhibit depletion of Ti. Slight/variable Th, Ce and P enrichment and Ti depletion are more pronounced in the more evolved Charnian lavas and diorites (Fig. 9a) and in the mostly intermediate volcaniclastic successions underlying the Worcester Graben (Fig. 9b). Evolved felsic compositions exhibit the greatest enrichment of Th (and other LILEs) and Ce, extreme depletion of P and Ti (Fig. 9c, d) and a negative Eu anomaly of increasing magnitude (Fig. 10c, d). These patterns are comparable with those of calc-alkaline or high-K calc-alkaline magmatic arcs (Pearce 1982) with a significant component of intracrustal melt.

The trends in magmatic evolution described here are compatible with the progressive development of a volcanic arc maturing from a primitive (island arc or marginal basin) to a more mature calc-alkaline or high-K calc-alkaline arc magmatic system (Pharaoh *et al.* 1987). The most primitive parental magmas are the island arc tholeiites found throughout the Charnian Domain, not restricted to the Charnwood and Warren House outcrops described by Pharaoh *et al.* (1987). They include the basaltic andesites penetrated by the Withycombe Farm borehole and the North Charnwood diorite. Undeformed mafic dykes (Figs 9c, 10c), which post-date the amphibolite facies metamorphism of the MPC, are compositionally similar. A component of additional enrichment in Uriconian lavas (Fig. 9d), identified by Pharaoh *et al.* (1987) as a possible lithospheric mantle component, is compatible with the presence of pre-Charnian crust to the west of the Malvern Lineament.

Although Charnian silicic rocks are relatively abundant in outcrop, they are deficient in Zr (typically <100 ppm). This is inferred to be a consequence of their formation via the fractionation of primitive island arc tholeiitic magma from a depleted mantle source (Pharaoh *et al.* 1987). Consequently, it is difficult to obtain sufficient zircon grains for U–Pb dating (Noble *et al.* 2015). The same is not true in areas to the west, where either extreme magmatic fractionation (Warren House Formation) or the presence of a sub-lithospheric mantle component (Uriconian volcanic suites) or a crustal contaminant have increased the content of Zr (and zircon). The question arises as to where the ferromagnesian cumulates resulting from this fractionation process reside because they are not exposed at the present level of crustal erosion.

The MORB-normalized geochemical patterns (Fig. 9) of the highly evolved felsic compositions (Warren House Formation, Uriconian volcanic suites) also bear witness to the strong depletion of P and Ti accompanied by the removal of siderophile elements (transition metals) such as Fe, Mn, Co, V and Zn. These geochemical characteristics are compatible with the removal of accessory minerals such as apatite (for P) and Fe-rich spinel as titanomagnetite (for Ti, Fe, Mn, V and Zn). These depletions are not observed in more primitive compositions (Fig. 9) and thus cannot be attributed to retention in the mantle source region. We infer that these accessory minerals were incorporated into tabular piles of mafic to intermediate cumulates on the floors of contemporary magma chambers.

The fractionation of Fe-rich spinel (or titanomagnetite) is thought to occur under conditions of high fO_2 (Osborn 1962). Zimmer *et al.* (2010) postulated that the presence of >2 wt% water (and, consequently, a high oxidation state) in a primary basaltic magma leads to the early crystallization of spinel (magnetite) and the suppression of plagioclase crystallization, resulting in the calc-alkaline trend of magmatic evolution. Under such conditions, ferromagnesian cumulate assemblages of bulk dioritic composition containing clinopyroxene, amphibole and a significant proportion of magnetite are the anticipated components of deep (>10 km) magma chambers. In Figure 10, late-stage differentiates show a small, but progressively increasing, negative Eu anomaly compatible with the fractionation of plagioclase. The formation of immiscible oxide liquids in the fractionated magma chambers, facilitated by the high content of volatiles such as Cl (Knipping *et al.* 2015), may also have played a part in the fractionation process.

Integrated petrogenetic and petrophysical interpretation

From the perspective of Ediacaran crustal evolution, the largest and most intensely modelled magnetic anomalies in the study region are the various components of the SCEMA. The geophysical model suggests that primitive subduction-related lavas in the Withycombe Farm borehole are possibly underlain by an Ediacaran ferromagnesian cumulate foundation in the mid- and lower crust. The presence of such cumulate material could balance the large volumes of silicic volcanic products observed at shallow crustal levels. The North Charnwood diorite is similar in both physical properties (Supplementary Publication 1, Table 1) and geochemistry (Supplementary Publication 2, Table 1) to the Withycombe basaltic andesite lava, reflecting a similar trend of magmatic evolution. The arc magmatic complex occupies an NNW-trending belt, *c.* 40 km wide, stretching 250 km from Wolverhampton in the north (where it is shallowest at 2.5–7 km depth) to the English south coast, where it is thicker and deeper.

The greatest MMS values are co-located with the deepest Moho (36–40 km or more) beneath the Midlands Microcraton in southern Britain (Ziegler and Dèzes 2006; Baykiev *et al.* 2018; Licciardi *et al.* 2020; Bonadio *et al.* 2021). The wedge-like geometry of the complex suggests that the magmatic rift propagated towards the north (in present day coordinates). The inferred location of the Charnian arc core shows good correspondence with the positive shear wave speed anomaly identified at 7–15 km depth by Bonadio *et al.* (2021). This positive anomaly is no longer visible by 30 km depth. However, it is present in the lithospheric depth range (90–170 km) (Bonadio *et al.*

2021). The attributes of the lithosphere beneath the microcraton may therefore have been established in the late Ediacaran. This explains its rigidity since the Cambrian (Pharaoh 2018).

A west–east-trending offset of the top of the SCEMA to south of the Variscan Front is not co-located with the thrust front identified from seismic reflection profiling and the edge of the gravity low, which is located 20–30 km (Fig. 7) farther north (e.g. Busby and Smith 2001). The amplitude of MA28 (Fig. 3) is apparently muted by the presence of 2–4 km of Mesozoic strata in the Wessex–Channel Basin, as well as by thin-skinned thrust nappes of the Variscide Rhenohercynian Zone (Busby *et al.* 1993; Busby and Smith 2001). Our modelling confirms the conclusion of these researchers that the SCEMA and SEMA are associated with the top of the magnetic Precambrian basement, which continues beyond the Variscan Front to the south coast of England. Figures 4c and 7b show that the area of the magnetic source is similar and likely increases in width across this tectonic boundary. The offset of the MMS *c.* 0.10 SI level is observed to be from *c.* 10 to 15 km depth (Figs 6, 7b) across the boundary and from *c.* 20 to 25 km at the MMS *c.* 0.035 SI level (Fig. 7d). A consistent vertical offset of *c.* 5 km is therefore inferred. The north–south sections (Fig. 6) show that the apparent dip of the interface is 20° to the south.

The magmatic arc associated with Charnian magmatism to the east of the Malvern and Cheltenham lineaments generated the shallow to deep crustal magnetic sources of the large SCEMA–SEMA set. We argue that the volume of magmatic rocks involved is compatible with severe attenuation of the lithosphere of the Marches Terrane across a distance of 80–100 km. The Charnian Domain can thus be regarded as a quasi-ensimatic arc, rather than a truly oceanic ensimatic arc. By contrast, the shallower magnetic sources for MA33 (Figs 3, 7a, b) are associated with Uriconian volcanic rocks erupted in ensialic rifts formed by smaller degrees of extension of the Marches Terrane. This interpretation is compatible with that from the Lithospheric Profile in Britain (LISPB)–DELTA seismic refraction data, where diffractions near the WBFS indicate the presence of steep faults bounding a rift-like structure to at least 10 km depth (Maguire *et al.* 2011). The Uriconian–Longmyndian volcano-sedimentary rift, along with other possible examples in Wales (e.g. the Llangynog Inlier, the St Davids, Pebidian and Johnston inliers in South Wales, and the Bryn-Teg borehole suite farther north, Fig. 1) are interpreted as probably coeval with Charnian rifting and magmatism, but are not strictly part of the Charnian Domain, which lies farther east (Fig. 2). Further systematic isotope studies are required to confirm this hypothesis. The western boundary of the Charnwood Terrane was previously taken at the Malvern Lineament (Pharaoh *et al.* 1987) and although this (with minor remapping) may be true in the north, our modelling work favours the Cheltenham Lineament as the western boundary of the Charnian Domain farther south. This interpretation attributes the crust underlying the western part of the Worcester Basin to the MPC, as suggested by previous modelling (Barclay *et al.* 1997).

This new conceptual framework for the Charnian Domain requires revision of the boundaries previously recognized for the Charnwood Terrane, as well as younger Paleozoic structures for which it forms a tectonic template. It has led to a minor remapping of the domain boundary towards the northern end of the Malvern Lineament and a more significant offset at the Cheltenham Lineament in the south. The relationship of the Charnian Domain to older crust in the Marches Terrane remains cryptic, but we argue that the domain most likely formed in an extensional rift, hosted by slightly older juvenile crust, rather than as part of an accretionary terrane mosaic. Comparison of representative geochemical data from the Charnian magmatic phase shows a continuum from depleted (island arc tholeiite) to enriched (high-K calc-alkaline basalt) magma types, reflecting increasing maturity of the arc system over time and, probably, in space (from east to west in present day coordinates).

The transitional crust of the Marches Terrane may also underlie the Charnian marginal basins – for example, beneath the Worcester Basin (an inferred back-arc basin) and in the 80 km wide region comprising Arvonian crust intersected by deep boreholes in eastern England (inferred forearc basin). Petrophysical log data suggest that the volcaniclastic strata intersected by boreholes in the Worcester Basin to west of the SCEMA represent the most evolved component of the Charnian magmatic phase. We suspect that the pervasive brown coloration observed in samples throughout these deep basement penetrations may reflect Ediacaran subaerial weathering within an emergent later stage of the back-arc basin. Deep weathering is compatible with the subtropical palaeolatitude for the Nuneaton area inferred by Vizan *et al.* (2003). The Warren House pillow lavas are interpreted to represent an earlier, more primitive stage of this back-arc basin. By contrast, Charnwood Forest may correspond to a deep-water forearc basin to the east of the arc.

The volcaniclastic successions of both the inferred forearc and back-arc basins are several kilometres thick and comprise repetitive, thick units of breccia chaotically emplaced as debris flows, as well as intervening finer grained successions deposited either by marine subaqueous gravity flow mechanisms or by subaerial pyroclastic flows and airfall. The Nuneaton quarry outcrop, the thickest exposed debrite (Carney and Pharaoh 1993; Carney 1995), lies on the eastern shoulder of the magmatic arc (Figs 1–3). The volcaniclastic rocks in the Hollowell borehole, located in the inferred forearc basin, lie at the eastern boundary of the Charnian Domain and the detritus is of Arvonian, rather than Charnian, affinity. The juxtaposed Arvonian crust here (encountered in the Orton and Glinton 1 boreholes) was the likely provenance of the *c.* 610 Ma zircon grains, both detrital and xenocrystic, in the Charnian strata and intrusions (Noble *et al.* 2015).

North-striking mafic dykes in the Malvern Hills and Charnwood and Nuneaton outcrops are interpreted by us as co-genetic with respect to Charnian magmatism. This interpretation is compatible with the presence of north-striking extensional faults in the same localities. The inferred internal structure of the arc (MA26, Figs 7, 8) also suggests roughly west–east extension (present day coordinates). The arc complex is either in steep (? faulted) contact with the marginal basins identified here or with the >50 Ma older crust of the Marches Terrane consolidated in the previous (Arvonian) episode of calc-alkaline magmatism. The correlation of the bifurcated anomaly MA26 with MA28 to the south of the Variscan Front (Fig. 7) is uncertain and various possibilities arise from the interpretation of the internal structure chosen. MA28 may therefore correspond to the axial region of MA26, which has undergone an additional phase of extension, or it may correlate with one of the magnetic ridges MA26W/MA26E.

The cause of MA34–MA35 in the London–Luton area (Fig. 3) is more difficult to interpret. Figures 4 and 7 emphasize the distinctive appearance of this source. The source of MA34–MA35 is poorly expressed at 10 km depth (Fig. 5a, b), has a simpler, tabular structure than the SCEMA and lacks the high MMS values characteristic of the SCEMA (Fig. 7). Among possible explanations for this contrast are that it represents a slightly earlier phase of Charnian rifting than the main SCEMA body, or that it reflects pre-Charnian, possibly Arvonian, magmatism. The former possibility is preferred and indicated on Figure 8. In either case, it seems unlikely that this distinctive basement block is transected by the concealed eastern boundary of the Midland microcraton and more likely follows Lineament 555L (the Saffron Walden Lineament) recognized by Cornwell and Walker (1989).

Minor offsets at west–east-trending lineaments occur in the West and South Midlands, at the Variscan Front, and at the English south coast, where the belt is truncated near the Purbeck–Wight Fault, overlying a likely Variscan terrane boundary (Figs 7, 8). The lineaments are observed to segment the SCEMA (e.g. Lee *et al.* 1990, 1991). The overall sense of offset on these lineaments is sinistral to the north of the Variscan Front and dextral to the south of it, which suggests that their final displacements may be of different ages: possibly latest Ediacaran or early Devonian (Acadian) to the north of the Variscan Front and late Carboniferous (Variscan) to the south of it. Another possibility is that the lineaments mark discrete stages in the northward propagation of the magmatic rift. The northern group of lineaments is oriented roughly parallel to the fold axial planes in the Charnian Supergroup outcrop (strike 100°), as well as the northern edge of MA34. These folds are transected by a cleavage striking 100–120° (Evans 1963) dated at 425–416 Ma (late Silurian to Early Devonian) by the $^{40}Ar–^{39}Ar$ method (Carney *et al.* 2008).

Taupo–Bay of Plenty volcanic province: a recent analogue for the Charnian Domain?

An important argument in favour of the terrane amalgamation hypothesis (Pharaoh *et al.* 1987) was its ability to explain the diversity of subduction-related magmatic types within a relatively small (200 km × 300 km) region of southern Britain. We now recognize that comparable magmatic diversity is present within the Quaternary Hikurangi subduction system (Fig. 11), encompassing the Kermadec Ridge, the Bay of Plenty, the Taupo volcanic zone (TVZ) and the Taranaki volcanic zone of North Island, New Zealand (Gamble *et al.* 1993). The southern end of the 1600 km long Tonga–Kermadec island arc system in the SW Pacific, and its projection into the juvenile continental crust of North Island, thus provide a potential analogue for the Charnian Domain.

New Zealand lies at the eastern edge of an extensive submarine continental area known as Zealandia (Mortimer *et al.* 2017), which extends to Australia. Some elements of this crust (the Buller and Takaka terranes) are relatively old, dating from the Ordovician and possibly the Mesoproterozoic, but it mostly comprises juvenile crust accreted in the Mesozoic, as exposed in South Island (Fig. 11). Within a 200 km × 400 km region, a range of magma types within the spectrum basalt–andesite–dacite–rhyolite, but also including some high-K andesites, has been generated by subduction magmatism. The key points of interest are:

- the topography/bathymetry of the trench and the crustal composition and thickness are well constrained;
- the deep geometry of the subduction zone and descending slab is known from seismological evidence and is comparatively simple (cf. other western Pacific subduction systems);
- the tectonic setting of any volcano within the arc magmatic system is well known;
- all of the volcanic products have been erupted within the last 2 Ma so that the chronology of magmatic events is well constrained and effectively contemporaneous; and
- a comprehensive geochemical and isotopic dataset is available for the unmetamorphosed lavas.

The Pacific plate is being subducted westwards under the Australian plate at a rate of *c.* 5 cm a^{-1} (Cole *et al.* 2000). Basalts and basaltic andesites collected from seamounts in the Kermadec Arc have low abundances (less than normal-type MORB) of HFSEs such as Ti, Zr, Nb, Ta and Hf (Gamble *et al.* 1993) (cf. the Withycombe Farm borehole and Warren House lavas). The magmatic arc crosses the continent–ocean divide (slope break) at *c.* 2000 m water depth, shallowing into the Bay of Plenty. The White Island composite stratovolcano sitting in 500 m of water (Cole *et al.* 2000) contributes significant volcaniclastic sediment to the surrounding basin as subaqueous debris flows. Basalts, andesites, dacites and rhyolites exhibit significant enrichment in LILEs, interpreted as a supra-

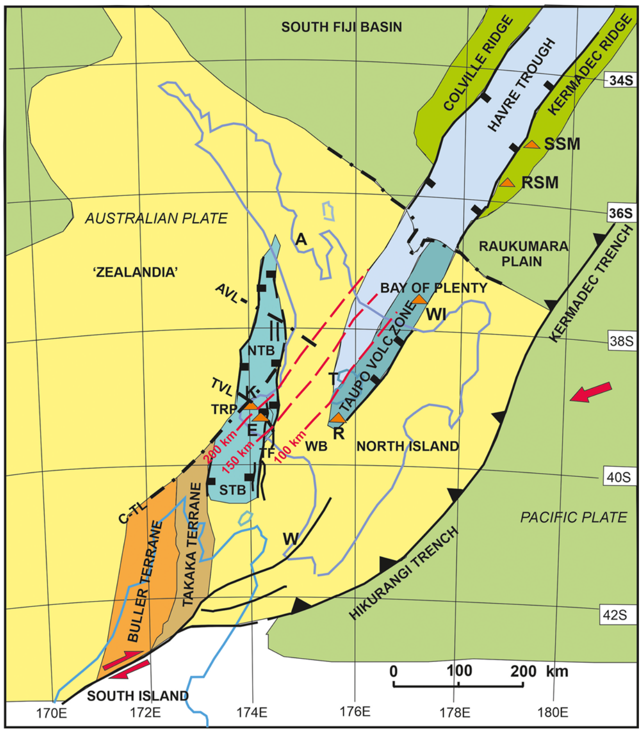

Fig. 11. Simplified geological map of North Island, New Zealand showing the key geological features: yellow, (?Mesoproterozoic, Paleozoic–Recent) crust of Zealandia Continent; orange, identified older (Paleozoic) crustal terranes within Zealandia (after Mortimer *et al.* 2017); blue, volcanic domains (Bay of Plenty, Taupo) and marginal basin/rifts (Taranaki; green, oceanic crust of Pacific plate; olive green, volcanic ridges. COB, continent–ocean boundary and seamount locations after Gamble *et al.* (1993). Key locations: A, Auckland; E, Egmont (Mt Taranaki) volcano; K, Kaitake volcano; R, Ruapehu volcano; RSM, Rumble seamounts; SSM, Silent seamounts; W, Wellington; WI, White Island volcano. Basin elements and lineaments after Price *et al.* (1999): AVL, Alexandria Volcanic Lineament; C-TL, Cook–Turi Lineament; NTB, North Taranaki Basin; STB, South Taranaki Basin; TF, Taranaki Fault; TRP, Taranaki Ring Plain; TVL, Taranaki Volcanic Lineament. Red contours (km) show depth to Wadati–Benioff Zone.

subduction zone component (Cole *et al.* 2000). The arc extends onshore as a series of stratovolcanoes in the TVZ, which is an extensional rift zone propagating southwards into juvenile crust in the back-arc region of the Hikurangi trench–arc system. The width of the forearc basin is between 150 and 200 km. The TVZ basalts have a higher content of HFSEs than most Kermadec basalts (Gamble *et al.* 1993), whereas the LILEs are strongly enriched compared with typical MORBs (cf. the Uriconian basalts). Mt Egmont lies *c.* 140 km west of the TVZ and is the latest in a series of four stratovolcanoes created along the Taranaki Volcanic Lineament in the Quaternary. The Taranaki magmas are generated in the subduction-enriched mantle wedge overlying the Wadati–Benioff zone of the Hikurangi system at a depth of *c.* 200 km and are possible analogues for evolved calc-alkaline basalts in the Charnian back-arc region. In a future orogeny, the TVZ and Taranaki lavas are more likely to be preserved than their counterparts in the oceanic and marginal basin components of the Hikurangi margin.

Discussion

Although the boundaries of the Charnian Domain are concealed and the relationship with the surrounding, slightly older (*c.* 720–600 Ma) crust of the host Marches Terrane remains cryptic, our model does not require severe tectonic modification of original extensional faults – for example, by terrane displacement in the

Ediacaran. Instead, the domain is inferred to have formed at *c.* 570–550 Ma as a supra-subduction rift basin with extreme attenuation (hyper-extension) of juvenile Ediacaran crust, splitting the Marches Terrane into forearc and back-arc segments. Using the Quaternary development of the Taupo Zone (New Zealand) as an analogue, this quasi-ensimatic rift wedge propagated northwards (present day coordinates) progressively with time and, in its most attenuated central and southern segments, the original sialic lower crust was entirely replaced by ferromagnesian cumulate material.

We continue to prefer an Ediacaran location for the Marches Terrane either within (or close to) the Amazonian margin of Gondwana. The limited available U–Pb upper intercept ages (Tucker and Pharaoh 1991) and T_{DM} model ages (Noble *et al.* 1993; Schofield *et al.* 2016) indicate inheritance from Mesoproterozoic and, more specifically, Rondonian crust (e.g. Willner *et al.* 2013). Such ages are rarely found in West African Gondwana and Grenville–Sveconorwegian ages, characteristic of Baltica and Laurentia, are apparently absent in southern England. Thus the Ediacaran palaeogeographical location for the Marches Terrane (East Avalonia) is different to that advocated for some parts of West Avalonia (Landing *et al.* 2022; Beranek *et al.* 2023; Murphy *et al.* 2023).

The assumed rift propagation direction appears to be inconsistent with a location on the northern margin of Gondwana and an inferred (?Iapetus or older) ocean lying to the north (e.g. Murphy 2007). It is, however, compatible with such a model if the domain underwent post-Ediacaran rotation. Vizan *et al.* (2003) recognized a negative Ediacaran declination in the palaeomagnetic data for the Nuneaton district, indicating a 165° clockwise rotation about a vertical axis since 565 Ma. This could have occurred when the crust of the Marches Terrane was rifted away from the Gondwana margin and incorporated in the East Avalonia Terrane during the Caledonian Orogeny (Soper *et al.* 1987). Thus the original propagation direction of the rift wedge in Ediacaran time may indeed have been from the north.

The Uriconian–Longmyndian and other possibly coeval volcano-sedimentary sequences in Wales result from the more limited extension of the Marches Terrane crust within ensialic rifts. In South Wales, the emplacement of part of the plutonic Johnston Complex has been precisely dated at 570 ± 3 Ma (Clarke *et al.* 2023), supporting this contention. The terms Charnwood Terrane and Wrekin Terrane are therefore redundant and it is recommended that their usage be discontinued. These volcanic suites simply reflect different degrees of extension within the same coeval arc magmatic system (cf. the TVZ and Taranaki volcanic zone of New Zealand). Within the Charnian Domain, juvenile arc/marginal basin crust lies to the east and high-K calc-alkaline magmatism is present in the west, suggesting a west-dipping subduction zone (present day coordinates) or east-dipping prior to the rotation inferred here.

The massive debrite unit in the Nuneaton outcrop perched on the eastern shoulder of the putative arc, more proximal than the Charnwood outcrop, suggests a regional palaeoslope towards the NE (present day orientation). This interpretation is compatible with observations of slump folds in Charnwood Forest, which suggest a palaeoslope towards the NNE, but not the inferred emplacement direction of the Sliding Stone Slump Breccia, which is towards the SE (Moseley and Ford 1985; Sutherland *et al.* 1987). The latter may reflect a local palaeoslope associated with the development of a penecontemporaneous extrusive lava dome.

Maps and cross-sections derived from the geophysical model image possible internal structures within the magmatic arc – in particular, the presence of a median rift and superimposed annular magnetic features in the inferred core region of the arc near Coventry and north and south of Oxford. We assume that the annular features are not artefacts of the modelling process because they recur throughout the domain. We speculate that these might represent the ghosts of fossilized magma chambers or caldera structures within the mid-crust beneath the arc core. We also imaged several west–east-trending lineaments with minor offsets that partition the arc along its length.

The source of the strong magnetic anomalies modelled in the mid- and lower crust remains a matter of speculation in the absence of evidence from xenoliths or seismic refraction data. Possible analogues include the thick (>35 km) piles of ferromagnesian cumulates in the lower and mid-crust of the obducted Kohistan island arc (Cretaceous, Himalaya) and the petrographically similar Talkeetna arc (Jurassic, Alaska) (Petterson 2010). The presence of ferromagnesian cumulate material associated with fractionated titanomagnetite in the lower crust of southern Britain might explain the apparent absence of Moho reflectivity (Chadwick *et al.* 1989). Another possibility is the presence of the iron oxide–apatite mineralization found associated with calc-alkaline complexes of Mesozoic–Holocene age in Chile and Mexico (Swanson *et al.* 1978) and of Paleoproterozoic age at Kiruna, Sweden (Frietsch 1978). The relative importance of magmatic v. hydrothermal processes in such deposits is, however, still much debated (e.g. Dare *et al.* 2014) and, although the association with calc-alkaline magmatic suites is interesting, none of these iron oxide–apatite deposits is on a crustal scale.

The development of the Marches Terrane from *c.* 720 to 600 Ma and the subsequent emplacement of the Charnian quasi-ensimatic wedge at 570–550 Ma created a laterally heterogeneous crust in southern Britain. The crust of the early Paleozoic Midlands Microcraton (and, subsequently, the Wales–Anglo–Brabant Massif and the London Platform) is anomalously thick with respect to the surrounding Caledonide–Variscide belts (e.g. Ziegler 1990), as well as lacking the highly reflective lower crust so typical of the latter (Chadwick *et al.* 1989). In our model, magnetic plutonic rocks of the Charnian arc foundation extend to at least 32 km depth, the inferred depth of the Curie temperature isotherm, and account for the anomalous geophysical signatures of the Midlands Microcraton. We argue that the persistent buoyant and rigid behaviour of the microcraton/massif observed throughout Phanerozoic time (Pharaoh 2018) was a consequence of this Ediacaran phase of heterogeneous crustal generation.

The relationship of Arvonian crust in North Wales to the Marches Terrane is an interesting question. Schofield *et al.* (2016, 2020) recognized that the felsic volcanic rocks of the Arvonian inliers and plutonic equivalents (Sarn Complex), occupy a distinct Arfon Terrane within the Menai Strait Fault System, incorporating disrupted elements of the Fenland Terrane. They also speculated that the boundary with the adjacent Cymru Terrane is concealed by Mid-Ordovician cover in Snowdonia. We support this contention and view the Arfon Terrane, together with exhumed slices of the lower plate of the Charnian phase subduction zone and components of a Cambrian deep-water continental margin (the Mona Complex), as allochthonous units displaced sinistrally a distance of at least 160 km from the eastern margin of the Marches Terrane (Fig. 1c) during Monian deformation in the early Ordovician (Schofield *et al.* 2008, 2020). We therefore argue that the Arfon Terrane has Avalonian, rather than Ganderian, affinity, as proposed by Schofield *et al.* (2020).

Conclusions

A holistic investigation of the Charnian Domain is underpinned by an integrated petrogenetic model driven by the inverse modelling of magnetic susceptibility using aeromagnetic potential field data and supported by field observations, borehole geophysical logs and whole-rock geochemical data. The study shows that the submarine volcano-sedimentary succession exposed in Charnwood and Nuneaton is probably unrepresentative of the magmatic arc system at depth. The geophysical model has been tomographically dissected to generate maps and vertical sections to visualize its internal magnetic structure. The model suggests that the source of the largest and most complex magnetic anomaly in southern Britain can be mapped into the lower crust and is coincident with the greatest Moho depth. Ferromagnesian crystal cumulates incorporating titanomagnetite are inferred to occupy a significant proportion of the mid- and lower crustal volume, implying the development of a hyper-extended, quasi-ensimatic rift. The extensive presence of cumulates in the lower crust could explain the apparent lack of a seismic reflection Moho and other anomalous geophysical attributes. The arc magmatic rift forms a wedge 150 km wide at the south coast of England and extends northwards as a prong into a shallower crustal level in the West Midlands near Wolverhampton. Further evidence of west–east extension at this time is recorded by north-striking dykes and faults in outcrop. The strongly anisotropic crustal model presented is amenable to testing by teleseismic and magnetotelluric investigations, which are well within existing capabilities.

The nature of the boundary between the Ediacaran Charnian Domain and the slightly older Cryogenian–Ediacaran crust attributed to the Marches Terrane host remains obscure, but more likely reflects extensional processes than subsequent terrane accretion/displacement tectonics. Variable degrees of lithospheric extension across the arc/marginal basin complex adequately explain the development of the quasi-ensimatic Charnian Domain and coeval ensialic rifts in the back-arc region of the Marches Terrane. Subduction-related magmas generated during the Charnian phase range from primitive (island arc tholeiite) through to more evolved (calc-alkaline basalt) magmas erupted at *c.* 570–550 Ma in a rather small region of southern Britain. Evidence for the fractionation of titanomagnetite and apatite in felsic differentiates of these magmas is inferred from their geochemical compositions. Volcaniclastic successions in the marginal basins flanking the Charnian arc domain to the west (the inferred back-arc basin beneath the Worcester Basin) and east (the inferred forearc basin of Charnwood) reflect the increasing maturity of arc magmatism with time. Further isotopic studies will be required to test aspects of the evolution of the Charnian arc system.

The heterogeneous crustal structure created in the Ediacaran has strongly influenced the initiation and subsequent behaviour of younger, co-located tectonic elements such as the Midlands Microcraton, the Wales–Anglo–Brabant Massif, the Worcester Basin and the London Platform. These elements are developed on a geometrical template reflecting the reactivation of the Ediacaran crustal structures and exhibit a Phanerozoic subsidence and uplift history strongly influenced by this unusual lithosphere. The lower crust of the region is anomalously thick and unreflective compared with that of Caledonian–Variscan crust elsewhere in Europe (Ziegler and Dèzes 2006).

Recognition of a possible present day analogue, from the Hikurangi destructive margin in North Island, New Zealand, lends support to the model presented here. This analogue is remarkably similar in terms of crustal evolution, volcanic style, geochemical variation and areal extent to the Charnian Domain and it is tempting to draw similar conclusions on the tectonic environment.

Scientific editing by Stephen Daly

Acknowledgements The fieldwork on which this paper was based was encouraged by Mike Le Bas of Leicester University. The late Tim Brewer of Leicester University supervised the geochemical analysis of most of the samples described herein. The provision of PETREL® software by Schlumberger Corp. significantly facilitated the modelling and visualization process. The geochemical diagrams were prepared using the IGPET software developed by Michael Carr at Rutgers State University, New Jersey. We thank numerous colleagues at the British Geological Survey – in particular, Nigel Smith, Jon Busby, Andy Chadwick and Bill Barclay – for discussions in the field and the office. Comments from Richard Haslam and Brendan Murphy greatly improved this paper. Reviews by John Waldron, Robin Strachan and Andrea Mills are gratefully acknowledged. This paper is published with the approval of the Executive Director, British Geological Survey (Natural Environment Research Council).

Author contributions **TCP**: conceptualization (lead), formal analysis (lead), investigation (lead), methodology (lead), software (equal), supervision (lead), validation (equal), visualization (lead), writing – original draft (lead), writing – review and editing (equal); **DB**: conceptualization (supporting), formal analysis (equal), methodology (equal), software (equal), validation (equal), writing – original draft (supporting), writing – review and editing (supporting); **JDOW**: investigation (supporting), software (equal), visualization (equal), writing – review & editing (supporting); **JNC**: investigation (supporting), validation (equal), writing – review and editing (supporting); **PRW**: investigation (supporting), validation (supporting), writing – review and editing (supporting).

Funding The work described here was carried out over 30 years, supported by the National Capability programme of the British Geological Survey, funded by the Natural Environment Research Council and, more recently, UK Research and Innovation. No specific grant was received from any other funding agency.

Competing interests The authors declare that they have no known competing financial interests or personal relationships that could have appeared to influence the work reported in this paper.

Data availability The data that support the findings of this study are available from the British Geological Survey, but restrictions apply to the availability of these data, which were used under license for the current study and so are not publicly available. Data are, however, available from the authors upon reasonable request and with permission of the British Geological Survey.

References

Allen, J.R.L. 1968. Precambrian rocks. C. The Nuneaton district. *In:* Sylvester-Bradley, P.C. and Ford, T.D. (eds) *The Geology of the East Midlands*. Leicester University Press, 15–19.

Allsop, J.M., Ambrose, K. and Elson, R.J. 1987. New data on the stratigraphy and geophysics in the area around Hollowell, Northamptonshire, provided by a coal exploration borehole. *Proceedings of the Geologists' Association, London*, **98**, 157–170, https://doi.org/10.1016/S0016-7878(87)80003-2

Barclay, W.J., Ambrose, K., Chadwick, R.A. and Pharaoh, T.C. 1997. *Geology of the Country Around Worcester*. Memoir of the British Geological Survey, Sheet 199 (England and Wales).

Baykiev, E., Guerri, M. and Fullea, J. 2018. Integrating gravity and surface elevation with magnetic data: mapping the curie temperature beneath the British Isles and surrounding areas. *Frontiers in Earth Sciences*, **6**, 1–19, https://doi.org/10.3389/feart.2018.00001

Beamish, D., Pharaoh, T.C. and Schofield, D.I. 2021. A crustal magnetic model of Britain obtained by 3D inversion. *Tectonophysics*, **814**, 228982, https://doi.org/10.1016/j.tecto.2021.228982

Beckinsale, R.D., Chadwick, R.A., Worssam, B.C. and Moorlock, B.S.P. 1986. The evolution of the Malvern Lineament [abstract]. *Philosophical Transactions of the Royal Society of London*, **A317**, 277, https://doi.org/10.1098/rsta.1986.0036

Beranek, L.P., Hutter, A.D. *et al.* 2023. New evidence for the Baltican cratonic affinity and Tonian to Ediacaran tectonic evolution of West Avalonia in the Avalon Peninsula, Newfoundland, Canada. *Precambrian Research*, **390**, 107046, https://doi.org/10.1016/j.precamres.2023.107046

BGS 1996. *The Tectonic Map of Britain, Ireland and Adjacent Areas. Sheet 1. 1:1 500 000 Scale*. British Geological Survey and Geological Survey of Ireland.

Bonadio, R., Lebedev, S. *et al.* 2021. Optimal resolution tomography with error tracking and the structure of the crust and upper mantle beneath Ireland and Britain. *Geophysical Journal International*, **226**, 2158–2188, https://doi.org/10.1093/gji/ggab169

Boynton, H.E. 1978. Fossils from the Precambrian of Charnwood Forest, Leicestershire. *Mercian Geologist*, **6**, 291–296.

Bridge, D.M., Carney, J.N., Lawley, R.S. and Rushton, A.W.A. 1998. *The Geology of the Country Around Coventry and Nuneaton*. Memoir of the British Geological Survey, Sheet 169 (England and Wales).

Busby, J.P. and Smith, N.J.P. 2001. The nature of the Variscan basement in southeast England: evidence from integrated potential-field modelling. *Geological Magazine*, **138**, 669–685, https://doi.org/10.1017/S0016756801005751

Busby, J.P., Kimbell, G.S. and Pharaoh, T.C. 1993. Integrated geophysical/geological modelling of the Caledonian and Precambrian basement of southern Britain. *Geological Magazine*, **130**, 593–604, https://doi.org/10.1017/S0016756800020896

Busby, J.P., Walker, A.S.D. and Rollin, K.E. 2006. *Regional Geophysics of South-East England. An Interactive Guide to the Subsurface Structure Based on Regional Gravity and Magnetic Data. V1.0 [CD-ROM]*. British Geological Survey.

Carney, J.N. 1995. Precambrian and Lower Cambrian rocks of the Nuneaton Inlier: a field excursion to Boon's and Hartshill quarries. *Mercian Geologist*, **13**, 189–198.

Carney, J.N. 2000*a*. Charnwood Forest. *Geological Conservation Review*, **20**, 19–52.

Carney, J.N. 2000*b*. Igneous processes within late Precambrian volcanic centres near Whitwick, north-western Charnwood Forest. *Mercian Geologist*, **15**, 7–28.

Carney, J.N. and Pharaoh, T.C. 1993. *Geology, chemistry and structure of Precambrian rocks in quarries north-west of Nuneaton*. British Geological Survey Technical Report **WA/93/94**.

Carney, J.N., Alexandre, P., Pringle, M.S., Pharaoh, T.C., Merriman, R.J. and Kemp, S.J. 2008. $^{40}Ar/^{39}Ar$ constraints on the age of deformational fabrics in Charnwood Forest, UK. *Geological Magazine*, **145**, 702–713, https://doi.org/10.1017/S0016756808004950

Chadwick, R.A., Pharaoh, T.C. and Smith, N.J.P. 1989. Lower crustal heterogeneity beneath Britain from deep seismic reflection data. *Journal of the Geological Society, London*, **146**, 617–630, https://doi.org/10.1144/gsjgs.146.4.0617

Chroston, P.N., Allsop, J.M. and Cornwell, J.D. 1987. New seismic refraction evidence on the origin of the Bouguer anomaly low near Hunstanton, Norfolk. *Proceedings of the Yorkshire Geological Society*, **46**, 311–319, https://doi.org/10.1144/pygs.46.4.311

Clarke, A.J.I., Kirkland, C.L. and Glorie, S. 2023. A detective duo of apatite and zircon geochronology for East Avalonia, Johnston Complex, Wales. *Journal of the Geological Society, London*, **180**, jgs2022-178, https://doi.org/10.1144/jgs2022-178

Cole, J.W., Thordarson, T. and Burt, R.M. 2000. Magma origin and evolution of White Island (Whakaari) Volcano, Bay of Plenty, New Zealand. *Journal of Petrology*, **41**, 867–895, https://doi.org/10.1093/petrology/41.6.867

Compston, W., Wright, A.E. and Toghill, P. 2002. Dating the late Precambrian volcanicity of England and Wales. *Journal of the Geological Society, London*, **159**, 323–339, https://doi.org/10.1144/0016-764901-010

Cornwell, J.D. 1992. *Geophysical Investigations in the Worcester District*. British Geological Survey Technical Report **WK/92/17**.

Cornwell, J.D. and Walker, A.S.D. 1989. Regional geophysics. *In:* Plant, J.A. and Jones, D.G. (eds) *Metallogenic Models and Exploration Criteria for Buried Carbonate-Hosted Ore Deposits – a Multidisciplinary Study in Eastern England*. Institution of Mining and Metallurgy and British Geological Survey, 25–52.

Cornwell, J.D., Smith, N.J.P. and Pharaoh, T.C. 1994. Discussion of: 'Source of the Bicester magnetic anomaly' by P. Kearey and A.M. Rabae. *Geological Journal*, **29**, 277–280, https://doi.org/10.1002/gj.3350290307

Dare, S.A.S., Barnes, S.-J. and Beaudoin, G. 2014. Did the massive magnetite 'lava flows' of El Laco (Chile) form by magmatic or hydrothermal processes? New constraints from magnetite composition by LA-ICP-MS. *Mineralium Deposita*, **50**, 607–617, https://doi.org/10.1007/s00126-014-0560-1

Dearnley, R. 1966. *Ignimbrites from the Uriconian and Arvonian*. *Bulletin of the Geological Survey of Great Britain*, **24**, 1–6.

Dunn, F.S., Liu, A.G. *et al.* 2021. The developmental biology of Charnia and the eumetazoan affinity of the Ediacaran rangeomorphs. *Science Advances*, **7**, 1–13, https://10.5523/bris.mukcdnafukgq2n8oljgarls23

Ellis, P.F. and Kearey, P. 1984. An investigation of the Reading–Newbury magnetic anomaly. *Journal of the Geological Society, London*, **141**, 349–356, https://doi.org/10.1144/gsjgs.141.2.0349

Evans, A.M. 1963. Conoidal folding and oblique structures in Charnwood Forest. *Proceedings of the Yorkshire Geological Society*, **34**, 67–79, https://doi.org/10.1144/pygs.34.1.67

Ford, T.D. 1958. Precambrian fossils from Charnwood Forest. *Proceedings of the Yorkshire Geological Society*, **31**, 211–217, https://doi.org/10.1144/pygs.31.3.211

Foster, D., Holliday, D.W., Jones, C.M., Owens, B. and Welsh, A. 1989. The concealed Upper Palaeozoic rocks of Berkshire and South Oxfordshire. *Proceedings of the Geological Association*, **100**, 395–407, https://doi.org/10.1016/S0016-7878(89)80057-4

Frietsch, R. 1978. On the magmatic origin of the iron ores of the Kiruna type. *Economic Geology*, **73**, 478–485, https://doi.org/10.2113/gsecongeo.73.4.478

Gamble, J.A., Smith, I.E.M., McCulloch, M.T., Graham, I.J. and Kokelaar, B.P. 1993. The geochemistry and petrogenesis of basalts from the Taupo Volcanic Zone, New Zealand and Kermadec Island Arc, S.W. Pacific. *Journal of Volcanology and Geothermal Research*, **54**, 265–290, https://doi.org/10.1016/0377-0273(93)90067-2

Gibbons, W. 1987. The Menai Strait Fault system: an early Caledonian terrane boundary in North Wales. *Geology*, **15**, 744–747, https://doi.org/10.1130/0091-7613(1987)15<744:MSFSAE>2.0.CO;2

Gibbons, W. 1990. Transcurrent ductile shear zones and the dispersal of the Avalon Superterrane. *Geological Society, London, Special Publications*, **51**, 407–423, https://doi.org/10.1144/GSL.SP.1990.051.01.27

Gibbons, W. and Horák, J.M. 1996. The evolution of the Neoproterozoic Avalonian subduction system: evidence from the British Isles. *GSA, Special Papers*, **304**, 269–280, https://doi.org/10.1130/0-8137-2304-3.269

Greig, D.C., Wright, J.E., Hains, B.A. and Mitchell, G.H. 1968. *Geology of the Country Around Church Stretton, Craven Arms, Wenlock Edge and Brown Clee*. Memoir of the British Geological Survey, Sheet 166 (England and Wales).

Harrison, R.K. 1974. *Sidewall Slices from Ultramar Well, Netherton*. Geological Survey of Great Britain Petroleum Department, Unpublished Report.

Horton, A., Poole, E.G., Williams, B.J., Illing, V.C. and Hobson, G.D. 1987. *Geology of the Country Around Chipping Norton*. Memoir of the British Geological Survey, Sheet 218 (England and Wales).

Kearey, P. 1991. A possible basaltic deep source of the south-central England magnetic anomaly. *Journal of the Geological Society, London*, **148**, 775–780, https://doi.org/10.1144/gsjgs.148.4.0775

Kearey, P. and Rabae, A.M. 1993. Source of the Bicester magnetic anomaly. *Geological Journal*, **28**, 191–203, https://doi.org/10.1002/gj.3350280209

Kenchington, C.G., Harris, S.I., Vixseboxsec, P.B., Pickupd, C. and Wilby, P.R. 2018. The Ediacaran fossils of Charnwood Forest: shining new light on a major biological revolution. *Proceedings of the Geologists' Association*, **129**, 264–277, https://doi.org/10.1016/j.pgeola.2018.02.006

Knipping, J.L., Bilenker, L.D. *et al.* 2015. The role of high volatile content in the formation of immiscible oxide liquids in fractionated magma chambers. *Geology*, **43**, 591–594, https://doi.org/10.1130/G36650.1

Landing, E., Keppie, J.D., Keppie, F.D., Geyer, G. and Westrop, S.R. 2022. Greater Avalonia – latest Ediacaran–Ordovician 'peribaltic' terrane bounded by continental margin prisms ('Ganderia', Harlech Dome, Meguma): review, tectonic implications, and palaeogeography. *Earth-Science Reviews*, **224**, 103863, https://doi.org/10.1016/j.earscirev.2021.103863

Le Bas, M.J. 1972. Caledonian igneous rocks beneath central and eastern England. *Proceedings of the Yorkshire Geological Society*, **39**, 71–86, https://doi.org/10.1144/pygs.39.1.71

Lee, M.K., Pharaoh, T.C. and Soper, N.J. 1990. Structural trends in central Britain from images of gravity and aeromagnetic fields. *Journal of the Geological Society, London*, **147**, 241–258, https://doi.org/10.1144/gsjgs.147.2.0241

Lee, M.K., Pharaoh, T.C. and Green, A.C. 1991. Structural trends in the concealed basement of Eastern England from images of regional potential-field data. *Annales de la Société Géologique de Belgique*, **T114**, 45–62.

Lelièvre, P.G., Oldenburg, D.W. and Williams, N.C. 2009. Integrating geological and geophysical data through advanced constrained inversions. *Exploration Geophysics*, **40**, 334–341, https://doi.org/10.1071/EG09012

Li, Y. and Oldenburg, D.W. 1996. 3-D inversion of magnetic data. *Geophysics*, **61**, 394–408, https://doi.org/10.1190/1.1443968

Licciardi, A., England, R.W., Agostinetti, P. and Gallagher, K. 2020. Moho depth of the British Isles: a probabilistic perspective. *Geophysical Journal International*, **221**, 1384–1401, https://doi.org/10.1093/gji/ggaa021

Linnemann, U., Herbosch, A., Liégois, J.-P., Pin, C., Gärtner, A. and Hofmann, M. 2012. The Cambrian to Devonian odyssey of the Brabant Massif within Avalonia: a review with new zircon ages, geochemistry, Sm–Nd isotopes, stratigraphy and palaeogeography. *Earth-Science Reviews*, **112**, 126–154, https://doi.org/10.1016/j.earscirev.2012.02.007

Liu, A.G., Kenchington, C.G. and Mitchell, E.G. 2015. Remarkable insights into the paleoecology of the Avalonian Ediacaran macrobiota. *Gondwana Research*, **27**, 1355–1380, https://doi.org/10.1016/j.gr.2014.11.002

Maguire, P.K., England, R. and Hardwick, A. 2011. LISPB DELTA, a lithospheric seismic profile in Britain: analysis and interpretation of the Wales and southern England section. *Journal of the Geological Society, London*, **168**, 61–82, https://doi.org/10.1144/0016-76492010-030

Molyneux, S.G. 1991. The contribution of palaeontological data to an understanding of the Early Palaeozoic framework of eastern England. *Annales de la Société Géologique de Belgique*, **T114**, 93–106.

Mortimer, N., Campbell, H.J., Tulloch, A.J., King, P.R., Stagpoole, V.M. and Wood, R.A. 2017. Zeaalandia: Earth's hidden continent. *GSA Today*, **27**, 27–35, https://doi.org/10.1130/GSATG321A.1

Moseley, J.B. and Ford, T.D. 1985. A stratigraphic revision of the Late Precambrian rocks of the Charnwood Forest, Leicestershire. *Mercian Geologist*, **10**, 1–18.

Murphy, J.B. 2007. The evolution of the Rheic Ocean. From Avalonian–Cadomian active margin to Alleghenian–Variscan collision. *GSA, Special Papers*, **423**, 413–436, https://doi.org/10.1130/SPE423

Murphy, J.B., Keppie, J.D., Dostal, J. and Nance, R.D. 1999. Neoproterozoic–early Paleozoic evolution of Avalonia. *GSA, Special Papers*, **336**, 253–266, https://doi.org/10.1130/0-8137-2336-1.253

Murphy, J.B., Nance, R.D. and Wu, L. 2023. The provenance of Avalonia and its tectonic implications: a critical reappraisal. *Geological Society, London, Special Publications*, **531**, https://doi.org/10.1144/SP531-2022-176

Nance, R.D. and Murphy, J.B. 1996. Basement isotopic signatures and Neoproterozoic paleogeography of Avalonian-Cadomian and related terranes in the circum-North Atlantic. *GSA, Special Papers*, **304**, 333–348, https://doi.org/10.1130/0-8137-2304-3.333

Noble, S.R., Tucker, R.D. and Pharaoh, T.C. 1993. Lower Palaeozoic and Precambrian igneous rocks from eastern England and their bearing on late Ordovician closure of the Tornquist Sea: constraints from U–Pb and Nd isotopes. *Geological Magazine*, **130**, 738–747, https://doi.org/10.1017/S0016756800023190

Noble, S.R., Condon, D.J., Carney, J.N., Wilby, P.R., Pharaoh, T.C. and Ford, T.D. 2015. U–Pb geochronology and global context of the Charnian Supergroup, UK: constraints on the age of key Ediacaran fossil assemblages. *GSA Bulletin*, **127**, 250–265, https://doi.org/10.1130/B31013.1

Osborn, E.F. 1962. Reaction series for subalkaline igneous rocks based on different oxygen pressure conditions. *American Mineralogist*, **47**, 211–226.

Pearce, J.A. 1982. Trace element characteristics of lavas from destructive plate boundaries. *In*: Thorpe, R.S. (ed) *Orogenic Andesites*. John Wiley and Son, 252–548.

Petterson, M.G. 2010. A review of the geology and tectonics of the Kohistan island arc, north Pakistan. *Geological Society, London, Special Publications*, **338**, 287–327, https://doi.org/10.1144/SP338.14

Pharaoh, T.C. 2018. The Anglo–Brabant Massif: persistent but enigmatic palaeo-relief at the heart of western Europe. *Proceedings of the Geologists' Association*, **129**, 278–328, https://www.sciencedirect.com/science/article/pii/S0016787818300294

Pharaoh, T.C. and Carney, J. 2000. Introduction. *In:*Carney, J., Horak, J.M. *et al.* (eds) *Precambrian Rocks of England and Wales*. Geological Conservation Review. Joint Nature Conservation Committee–Chapman and Hall, 1–18.

Pharaoh, T.C. and Evans, C.J. (compilers) 1987. *Morley Quarry No. 1: Geological Well Completion Report*. Investigation of the Geothermal Potential of the UK. BGS Open File Report.

Pharaoh, T.C. and Gibbons, W.A. 1994. Precambrian rocks in England and Wales south of the Menai Strait Fault System. *Geological Society of London, Special Report*, **22**, 85–97, https://doi.org/10.1144/SR22.10

Pharaoh, T.C., Webb, P., Thorpe, R.S. and Beckinsale, R.D. 1987. Geochemical evidence for the tectonic setting of late Proterozoic volcanic suites in the central UK. *Geological Society, London, Special Publications*, **33**, 541–552, https://doi.org/10.1144/GSL.SP.1987.033.01.36

Pharaoh, T.C., Lee, M.K., Evans, C.J., Brewer, T.S. and Webb, P.C. 1991. A cryptic late Proterozoic island-arc and marginal basin complex in the heart of England. *Terra Abstracts*, **3**, 58.

Poole, E.G. 1978. Stratigraphy of the Withycombe Farm Borehole, near Banbury, Oxfordshire. *Bulletin of the Geological Survey of Great Britain*, **6**.

Price, R.C., Stewart, R.B., Woodland, J.D. and Smith, I.E.M. 1999. Petrogenesis of high-K arc magmas: evidence from Egmont Volcano, North Island, New Zealand. *Journal of Petrology*, **40**, 167–197.

Reedman, A.J., Leveridge, B.E. and Evans, R.B. 1984. The Arfon Group ('Arvonian') of North Wales. *Proceedings of the Geologists' Association*, **95**, 313–321, https://doi.org/10.1016/S0016-7878(84)80062-0

Rushton, A.W.A. and Molyneux, S.G. 1990. The Withycombe Formation (Oxfordshire subcrop of early Cambrian age). *Geological Magazine*, **127**, 363, https://doi.org/10.1017/S0016756800014928

Saunders, A.D. and Tarney, J. 1984. Geochemical characteristics of basaltic volcanism within back-arc basins. *Geological Society, London, Special Publications*, **16**, 59–76, https://doi.org/10.1144/GSL.SP.1984.016.01.05

Schofield, D.I., Evans, J.A., Millar, I.L., Wilby, P. and Aspden, J.A. 2008. New U–Pb and Rb–Sr constraints on pre-Acadian tectonism in North Wales. *Journal of the Geological Society, London*, **165**, 891–894, https://doi.org/10.1144/0016-76492008-044

Schofield, D.I., Millar, I.L., Wilby, P.R. and Evans, J.A. 2010. A new, high precision U–Pb date from the oldest known rocks in southern Britain. *Geological Magazine*, **147**, 145–150, https://doi.org/10.1017/S001675680999063X

Schofield, D.I., Potter, J., Barr, S.M., Horak, J.M., Millar, I.L. and Longstaffe, F.J. 2016. Reappraising the Neoproterozoic 'East Avalonian' terranes of southern Great Britain. *Gondwana Research*, **35**, 257–271, https://doi.org/10.1016/j.gr.2015.06.001

Schofield, D.I., Leslie, A.G., Wilby, P.R., Dartnall, R., Waldron, J.W.F. and Kendall, R.S. 2020. Tectonic evolution of Anglesey and adjacent mainland North Wales. *Geological Society, London, Special Publications*, **503**, 371–390, https://doi.org/10.1144/SP503-2020-9

Shail, R.K. and Leveridge, B.E. 2009. The Rhenohercynian passive margin of SW England: development, inversion and extensional reactivation. *Comptes Rendus Geoscience*, **341**, 140–155.

Smith, N.J.P. 1987. The deep geology of central England: the prospectivity of the Palaeozoic rocks. *In:* Brooks, J. and Glennie, K. (eds) *Petroleum Geology of Northwest Europe*. Graham & Trotman, 217–224.

Smith, N.J.P., Kirby, G.A. and Pharaoh, T.C. 2005. *The Structure and Evolution of the South-West Pennine Basin and Adjacent Area.* British Geological Survey, Subsurface Memoir.

Soper, N.J., Webb, B.C. and Woodcock, N. 1987. Late Caledonian (Acadian) transpression in north-west England: timing, geometry and geotectonic significance. *Proceedings of the Yorkshire Geological Society*, **46**, 175–192, https://doi.org/10.1144/pygs.46.3.175

Strachan, R.A., Nance, R.D., Dallmeyer, R.D., D'Lemos, R.S., Murphy, J.B. and Watt, G.R. 1996. Late Precambrian tectonothermal evolution of the Malverns Complex. *Journal of the Geological Society, London*, **153**, 589–600, https://doi.org/10.1144/gsjgs.153.4.0589

Strachan, R.A., Collins, A.S., Buchan, C., Nance, R.D., Murphy, J.B. and D'Lemos, R.S. 2007. Terrane analysis along a Neoproterozoic active margin of Gondwana: insights from U–Pb zircon geochronology. *Journal of the Geological Society, London*, **164**, 57–60, https://doi.org/10.1144/0016-76492006-014

Sutherland, D.S., Boynton, H.E., Ford, T.D., Le Bas, M.J. and Moseley, J. 1987. A guide to the geology of the Precambrian rocks of Bradgate Park in Charnwood Forest, Leicestershire. *Transactions of the Leicester Literary & Philosophical Society*, **81**, 47–83.

Swanson, E.R., Keizer, R.P., Lyons, J.L. and Clabaugh, S.E. 1978. Tertiary volcanism and caldera development near Durango City, Sierre Madre Occidental, Mexico. *GSA Bulletin*, **89**, 1000–1012, https://doi.org/10.1130/0016-7606(1978)89<1000:TVACDN>2.0.CO;2

Thorpe, R.S. 1974. Aspects of magmatism and plate tectonics in the Precambrian of England and Wales. *Geological Journal*, **9**, 115–135, https://doi.org/10.1002/gj.3350090202

Thorpe, R.S., Beckinsale, R.D., Patchett, P.J., Piper, A., Davies, G.R. and Evans, J.A. 1984. Crustal growth and late Precambrian–early Palaeozoic plate tectonic evolution of England and Wales. *Journal of the Geological Society, London*, **141**, 521–536, https://doi.org/10.1144/gsjgs.141.3.0521

Tucker, R.D. and Pharaoh, T.C. 1991. U-Pb zircon ages of late Precambrian igneous rocks in southern Britain. *Journal of the Geological Society, London*, **148**, 435–443, https://doi.org/10.1144/gsjgs.148.3.0435

Vizan, H., Carney, J.N., Turner, P., Ixer, R.A., Tomasso, M., Mullen, R.P. and Clarke, P. 2003. Late Neoproterozoic palaeogeography of Avalonia: some palaeomagnetic constraints from Nuneaton, central England. *Geological Magazine*, **140**, 685–705, https://doi.org/10.1017/S001675680300832X

Whittaker, A. 1980. *Kempsey No. 1*. Deep Geology Unit, Institute of Geological Sciences. Geological Well Completion Report **80/1**.

Whittaker, A., Holliday, D.W. and Penn, I.E. 1985. *Geophysical Logs in British Stratigraphy*. Geological Society, London, Special Reports, **13**.

Wilby, P.R., Carney, J.N. and Howe, M.A. 2011. A rich Ediacaran assemblage from eastern Avalonia: evidence of early widespread diversity in the deep ocean. *Geology*, **39**, 655–658, https://doi.org/10.1130/G31890.1

Williams, H. and Hatcher, R.D. 1982. Suspect terranes and accretionary history of the Appalachian Orogen. *Geology*, **10**, 530–536, https://doi.org/10.1130/0091-7613(1982)10<530:STAAHO>2.0.CO;2

Willner, A.P., Barr, S.M., Gerdes, A., Massonne, H.-J. and White, C.E. 2013. Origin and evolution of Avalonia: evidence from U–Pb and Lu–Hf isotopes in zircon from the Mira Terrane, Canada and the Stavelot–Venn Massif, Belgium. *Journal of the Geological Society, London*, **170**, 769–784, https://doi.org/10.1144/jgs2012-152

Wills, L.J. 1978. *A Palaeogeological Map of the Lower Palaeozoic Floor Below the Cover of Upper Devonian, Carboniferous and Later Formations with Inferred and Speculative Reconstructions of Lower Palaeozoic and Precambrian Outcrops in Adjacent Areas*. Geological Society, London, Memoirs, **8**.

Wills, L.J. and Shotton, F. 1934. New sections showing the junction of the Cambrian and Pre-Cambrian at Nuneaton. *Geological Magazine*, **71**, 512–521, https://doi.org/10.1017/S0016756800094917

Woodcock, N.H. 1991. The Welsh, Anglian and Belgian Caledonides compared. *Annales de la Société Géologique de Belgique*, **T114**, 5–17.

Woodcock, N.H. and Gibbons, W. 1988. Is the Welsh Borderland fault system a terrane boundary? *Journal of the Geological Society, London*, **145**, 915–933, https://doi.org/10.1144/gsjgs.145.6.0915

Worssam, B.C. and Old, R.A. 1988. *Geology of the Country Around Coalville. Memoir for the 1:50 000 Geological Sheet 155 (England and Wales)*. HMSO.

Ziegler, P.A. 1990. *Geological Atlas of Western and Central Europe*. 2nd edn. Shell International Petroleum.

Ziegler, P.A. and Dèzes, P. 2006. Crustal evolution of Western and Central Europe. *Geological Society, London, Memoirs*, **32**, 43–56, https://doi.org/10.1144/GSL.MEM.2006.032.01.03

Zimmer, M.M., Plank, T. *et al.* 2010. The role of water in generating the calc-alkaline trend: new volatile data for Aleutian magmas and a new tholeiitic index. *Journal of Petrology*, **51**, 2411–2444, https://doi.org/10.1093/petrology/egq062